Rep. Prog. Phys. **60** (1997) 1351–1396. Printed in the UK PII: S0034-4885(97)07903-7

Parity violation in atoms

Marie-Anne Bouchiat† and Claude Bouchiat‡

† Laboratoire Kastler-Brossel§, 24 rue Lhomond, 75231 Paris Cedex 05, France
‡ Laboratoire de Physique Théorique de l'École Normale Supérieure‖, 24 rue Lhomond, 75231 Paris Cedex 05, France

Received 1 August 1997

Abstract

Optical experiments have demonstrated cases in which mirror symmetry in stable atoms is broken during the absorption or emission of light. Such results, which are in conflict with quantum electrodynamics, support the theory of unification of the electromagnetic and weak interactions. The interpretation of the experimental results is based on exchanges of weak neutral Z_0 bosons between the electrons and the nucleus of the atom. A concise review of these phenomena in atomic physics is presented. The role of precise caesium parity-violation experiments, as a source of valuable information about electroweak physics, is illustrated by examples pertaining to experimental conditions which, in some cases, are not accessible to accelerator experiments. We give the basic principles of experiments, some under way and others completed, where a quantitative determination of the nuclear weak charge, Q_W, which plays for the Z^0 exchange the same role as the electric charge for the Coulomb interaction is to be, or has been achieved. In the most recent and most precise experiment the accuracy on Q_W is limited to 1% by the uncertainty due to atomic physics calculations. Such a result challenges specialists in atomic theory and nuclear structure, since a more accurate determination of Q_W would mean more stringent constraints upon possible extensions of the standard model. Moreover, clear evidence has recently been obtained for the existence of the nuclear anapole moment, which describes the valence electron interaction with a chiral nuclear-magnetization component induced by the parity-violating nuclear forces. In writing this review, our hope was to make clear that any improvement in atomic parity-violation measurements will allow the exploration of new areas of electroweak physics.

§ Unité de Recherche Associée au Centre National de la Recherche Scientifique, à l'École Normale Supérieure et à l'Université Pierre et Marie Curie.
‖ Unité Propre du Centre National de la Recherche Scientifique, associée à l'École Normale Supérieure et à l'Université de Paris-Sud.

0034-4885/97/111351+46$59.50

Contents

1. Introduction 1353
   - 1.1. Conservation and violation of parity in classical physics 1353
   - 1.2. Parity in quantum mechanics. Historical survey 1354
   - 1.3. The origin of parity violation in atoms 1355
   - 1.4. Non-conservation of P with T conservation 1356
   - 1.5. Parity violation in stable atoms and in nuclear physics: different physical origins and different orders of magnitude 1357
   - 1.6. Main questions addressed in this review 1358
2. Possible manifestations of parity violation in atomic and molecular physics 1359
   - 2.1. Different PNC tests 1359
   - 2.2. Coulomb versus electroweak electron–nucleus potential 1360
   - 2.3. The difficulty of detecting electroweak processes in atoms 1361
   - 2.4. Enhancement mechanisms 1362
   - 2.5. Energy shifts due to parity-violating electron–nucleus interaction in chiral molecules 1365
3. Parity-violation measurements in atomic radiative transitions 1368
   - 3.1. Where to search for parity violation in atomic physics 1368
   - 3.2. Optical rotation experiments 1369
   - 3.3. Stark experiments in forbidden M_1 transitions of Cs and Tl 1370
   - 3.4. The presently most accurate PNC experiment 1374
4. The results in caesium and their implications 1376
   - 4.1. Atomic physics calculations and the present status of the results in caesium 1376
   - 4.2. Implications for electroweak theory 1378
   - 4.3. The nuclear spin-dependent electron-nucleus PV interaction 1381
5. A new generation of experiments in progress and plans for future projects 1385
   - 5.1. The new Paris experiment in the $6S_{1/2} \rightarrow 7S_{1/2}$ Cs transition based on detection via stimulated emission 1386
   - 5.2. Search for parity violation in a string of isotopes belonging to the same element 1388
   - 5.3. Search for parity violation on a single trapped Ba^+ ion 1390
   - 5.4. Prospects for PNC measurements in relativistic hydrogenic ions and high-Z helium-like ions 1391
   - 5.5. An experimental project to search for an energy difference between two enantiomer molecules 1392
6. Conclusion 1392

Acknowledgment 1393

References 1393

1. Introduction

The concepts of parity conservation and parity violation cannot be considered as intuitive. Indeed, the effects of parity violation do not belong to our everyday experience and there are large domains of physics where the question of parity conservation is never addressed although it concerns one of the most elementary symmetry properties, mirror symmetry i.e. the symmetry with respect to a plane. Moreover, the denomination of parity traditionally given, does not contribute by itself to a straightforward understanding of the subject. Nevertheless, it becomes perfectly clear if one has in mind the context of the discovery of parity violation. Therefore in this introduction we shall first clarify the meaning of synonym expressions such as 'mirror symmetry breaking', 'parity non-conservation' (PNC) and 'parity violation' (PV) and we shall present a short historical survey.

1.1. Conservation and violation of parity in classical physics

Many objects, natural or artificial, exist in two different forms, each one being identical to the mirror image of the other. We can speak about the left-handed and the right-handed configurations of such objects. By reference to the left and the right hands which represent a typical example, all the objects endowed with such a handedness are said to be chiral (from Greek *kheir* = hand). Another example is that of chiral molecules: the left- and right-handed species (the so-called enantiomers) differ by the geometrical arrangement of the atoms inside the molecule: this arrangement is chiral. Such molecules share many identical physical properties (mass, absorption spectrum, water solubility . . .) but they differ as regards those involving their handedness, for instance their rotatory power, i.e. the rotation of the plane of polarization of light transmitted through a gas or a solution of these molecules. The optical rotation is opposite for the two species. If we observe a left-handed molecule and measure its optical rotation, in a mirror we see a right-handed molecule which has an opposite optical rotation, hence the same optical rotation as a right-handed molecule in the real world. We see that the optical rotation of a chiral molecule is a property which preserves mirror symmetry and we say that it is parity conserving.

In this review article we are going to deal with physical systems whose chiral property arises not from the spatial arrangement of the constituents, but from the interactions between the constituents which favour one orientation of the physical space with respect to the other. It is no longer the spatial arrangement which is chiral rather the physical interaction. Let us illustrate this with an example. For individual atoms there is no geometrical handedness. Any handedness in an ensemble of atoms must be imposed from the outside, for instance by applying an external magnetic field to the atoms or by giving them some preferred orientation of their spin. Without such an externally imposed handedness the atoms seen in a mirror are identical to those observed in real life. Let us suppose that in such conditions we study the absorption of circularly polarized light by a collection of atoms and find that only the left-circularly polarized photons are absorbed. This would mean that in a mirror we would see atoms absorbing only right-polarized photons, that is, the opposite of the real case. Such a situation would correspond to an extreme case of parity violation taking place in the interaction of light with the atoms. We all know that in actual fact this does not happen. We have all learnt in our textbooks that in absence of magnetic fields left- and right-circularly polarized photons interact identically with (unoriented) atoms. In the last 15 years, however, it has been proved by independent, very careful experiments that the processes of emission and absorption of photons by atoms manifest a slight preference for left- and right-circularly polarized photons or more generally a preference for a given

orientation of physical space. The observed effects are in fact very small, i.e. the difference of probabilities between two processes of opposite handedness is at the level of only 10^{-5} or 10^{-6}, in the special cases where it has been observed. Nevertheless, they represent unquestionable manifestations of parity violation in atomic physics. As tiny as they may be, the very existence of such parity-violation effects are in complete contradiction with the well established laws of the electrodynamics. They actually reveal the existence in atoms of a second interaction which was ignored before the 1970s. Until that time the atom was regarded as a system governed only by the electromagnetic interaction, an interaction entirely indifferent to the distinction between left and right. The present review outlines the experiments performed to measure parity violation (also called parity non-conservation) in atomic radiative transitions and analyses their implications.

1.2. Parity in quantum mechanics. Historical survey

In quantum mechanics it is customary to speak about space reflection rather than mirror symmetry. Space reflection to which corresponds the quantum mechanical operator parity P, is defined as the transformation in which each point of space $\boldsymbol{r}$ is transformed into its opposite $-\boldsymbol{r}$. We must note that a space reflection is nothing but the product of a symmetry with respect to a plane by a rotation around an axis perpendicular to this plane. Since this latter transformation does not modify all known physical interactions, space inversion and mirror symmetry are two physically equivalent transformations.

A PV measurement in atomic transitions implies that space reflection symmetry is broken by atomic forces. In quantum mechanics P can be viewed as the operator which transforms a given quantum state into its mirror image ($P^2 = 1$). A parity quantum number $\epsilon_P = \pm 1$ characterizes quantum states which coincide with their mirror images. As an illustration, let us consider the simple example of a non-relativistic particle in a central potential $V(r)$. The state vector $|\Psi\rangle$ is described by a wavefunction $\psi(\boldsymbol{r})$. The wavefunction of the mirror state $|\tilde{\Psi}\rangle = P|\Psi\rangle$ is given by $\tilde{\psi}(\boldsymbol{r}) = \psi(-\boldsymbol{r})$. A less trivial example is the case of a system of N independent electrons, given by the Hartree–Fock atomic model: $|\Psi\rangle = \prod_{i=1}^{i=N} \psi_{n_i l_i m_i}(\boldsymbol{r})$. As can be easily verified by writing $\tilde{\psi}(\boldsymbol{r}_1, \ldots \boldsymbol{r}_i, \ldots) = \psi(-\boldsymbol{r}_1, \ldots, -\boldsymbol{r}_i, \ldots)$ the parity quantum number ϵ_P of a system of N independent electrons is the product of the N individual quantum numbers $\epsilon_{P_i} = (-1)^{l_i}$. Consequently, we are led to say that the parity quantum number ϵ_P is a multiplicative quantum number. This contrasts with the magnetic quantum number associated with the projection of the angular momentum on the quantification axis which is an additive quantum number. If in a transition the products of the parity quantum numbers of the initial and final sub-systems are identical we say that parity is conserved. In this context the denomination of parity violation becomes perfectly clear. The conservation of an additive quantum number leads, in the classical limit, to a law of conservation for the corresponding classical quantity, such as, for instance, the angular momentum. By contrast, there is no equivalent correspondence for the multiplicative parity quantum number. This is why the concept of parity conservation is somewhat less intuitive than the notion of angular momentum conservation.

The first indication that parity conservation may not be universal goes back to the early 1950s. Pions and K mesons are spin-0 particles, considered today as bound quark–antiquark states. At that time, pions were known to have negative parity $\epsilon_\pi = -1$. The puzzle was then that the K meson was found to decay sometimes into two pions and sometimes into three pions, i.e. into two different final states of opposite parity. In a brilliant analysis, Lee and Yang (1956), showed that one had to face the following alternatives: either parity is not conserved in the decay, or the K meson is a parity doublet, i.e. a two-component state

of opposite parities. They noted that there was at that time no experimental evidence for parity conservation in transitions which, like the K decay, were induced by weak interactions. They devised new rules to test parity conservation in processes where the initial and final states have not necessarily well defined parities. We shall prove formally later (see section 2.1) by using simple quantum mechanical considerations that these rules are also direct consequences of the fact that the Hamiltonian which governs the system contains two parts, one which is even under mirror symmetry and the other which is odd.

The basic principle of most parity non-conservation experiments is to compare the rate of a given transition between two states, A and B, with the transition rate between their mirror states, $\tilde{A}$ and $\tilde{B}$. The experimental outcome is conveniently characterized by the difference between these rates divided by their sum, the so-called left–right asymmetry, A_{LR}. The measurement of a non-zero value of A_{LR} constitutes unambiguous evidence for parity violation in the transition. We note that A_{LR} is a pseudoscalar quantity, i.e. it is invariant under space rotation but changes sign under mirror reflection. This leads to a golden rule for the design of PV tests: define a pseudoscalar quantity built from the external fields used in the experiment and the observables measured. The measurement of a non-zero value constitutes a PV test. As early as 1957, Wu (1957) and her collaborators performing the first experiment of this type, actually followed this rule to observe a PV effect. This experiment was performed on ^{60}Co nuclei whose spins $\boldsymbol{I}$ were oriented. In the β decay of the nuclei it was observed that the probability for an electron to be emitted with a given momentum $\boldsymbol{p}$ involves a large contribution proportional to the scalar product $\langle \boldsymbol{I} \rangle \cdot \boldsymbol{p}$. (In simple terms, the electrons are emitted preferentially in the direction opposite to the orientation of the ^{60}Co nuclei.) Since $\boldsymbol{I}$ is an angular momentum, i.e. an axial vector, the quantity $\langle \boldsymbol{I} \rangle \cdot \boldsymbol{p}$ is actually a pseudoscalar and its presence in the transition probability manifests parity violation.

Many experiments followed and it was soon established that the weak interactions which, *inter alia*, are at the origin of the nuclei β decays, give rise to a breaking of the left–right symmetry of the physical space. But the effect of parity violation in radiative atomic transitions that we have already mentioned takes place in stable atoms and until the early 1970s, it was believed that the radiative transitions involving atoms having a stable nucleus should not exhibit a similar behaviour.

1.3. The origin of parity violation in atoms

The violation of parity in β decay is accompanied by a change in the electric charge of the decaying neutron. Until the 1970s all processes observed involving weak interactions were accompanied by an exchange of electric charge between the interacting particles and hence by a modification of their identity. These transformations are brought about by the particles that mediate the weak interaction, which belong to the family of particles called gauge bosons. The gauge bosons that mediate the weak interactions are analogous to the photons that mediate the electromagnetic interaction. Unlike the photon, however, which is electrically neutral, the gauge bosons W^+ and W^- that mediate all weak interactions known before 1970 carry a unit of electric charge. It was therefore taken for granted that the weak interaction and its associated parity violation were not relevant to the physics of the stable atom. Indeed, in order to ensure the stability of an atom the interaction must necessarily preserve the identity of the interacting particles.

The theoretical understanding of weak interactions was mathematically unsatisfactory until the late 1960s, when a new theory was proposed. Glashow (1961), Weinberg (1967) and Salam (1968) suggested independently that the weak interaction and the

electromagnetic interaction could be understood as different manifestations of a single, underlying interaction: the electroweak interaction (Itzykson and Zuber 1980). The unified electroweak theory was subsequently shown by 't Hooft to be amenable to a perturbation treatment in the same way as quantum electrodynamics ('t Hooft 1971a, b). The calculations of higher-order effects had invaluable implications: for instance they permitted an evaluation of the top quark mass even before its direct observation at the Fermi Laboratory.

An important prediction of the theory was the existence of a new gauge boson, the Z^0 that mediates a new kind of weak interaction. Both the $W^{\pm}$ and Z^0 bosons are results of the unification of the electromagnetic and weak interactions in the standard model. Because of this kinship, the Z^0 is expected to exhibit a chiral behaviour (i.e. it changes its coupling to constituents of matter particles when reflected in a mirror). But because the Z^0 particle carries no electric charge, the interactions do not lead to a change in the identity of the interacting particles. Indeed, the Z_0 is coupled to the fundamental matter constituents, electron, quark, etc, in two different ways: first, like a photon; indeed the Z_0 can then be viewed as a kind of heavy photon; secondly, like a pseudovector particle, which means more concretely that the coupling of the Z_0 to the electron is proportional to the electron helicity h_e, defined as the scalar product of the spin of the electron by its velocity: $h_e = \boldsymbol{\sigma}_e \cdot \boldsymbol{v}_e$. Like the circular polarization of the photon, the helicity h_e is odd under space reflection. This double-faceted feature of the Z_0 coupling to matter, implies that the Z_0 exchange electron–nucleus potential contains a part which is odd under space reflection. In the contribution proportional to h_e, which turns out to play the dominant role in atoms, the Z_0 coupling to the nucleus is similar to that of the photon.

By analogy with the nuclear electric charge, one is led to introduce *the weak charge of the nucleus* Q_W (Bouchiat and Bouchiat 1974a). Unlike the Coulomb potential, however, the chiral electron–nucleus interaction has a range very short compared to atomic size. As a consequence, its strength is given by the electron density near the nucleus times $h_e Q_W G_F$. The Fermi constant G_F clearly indicates the close connection with β decay. The weak charge Q_W plays the role of the fundamental constant of the atomic electroweak chiral interaction which is at the origin of this remarkable fact: the inert matter of the world we are living in is endowed with a spatial orientation.

1.4. Non-conservation of P with T conservation

Another important symmetry in physics is time reversal symmetry (to which corresponds the quantum mechanical operator T). We do not intend to discuss here in full generality the breaking of this symmetry. However, one must be aware that depending on whether a PNC interaction is invariant or not under T reversal, the physical effects which can manifest PNC present considerable differences. It is a consequence of the standard model that the weak interactions associated with Z^0 and $W^{\pm}$ exchanges are T conserving. Consequently, the pseudoscalar quantities which can manifest their presence are necessarily *even* under the application of the operator T. However, it should be stressed that this rule is valid only if the transition rates can be calculated in the Born approximation, which turns out to be the case for the processes considered here. For instance, it is easily verified that the pseudoscalar $\boldsymbol{I} \cdot \boldsymbol{p}$ which revealed PNC in Wu's experiment satisfies this rule, since both $\boldsymbol{I}$ and $\boldsymbol{p}$ change sign in the operation which changes t into $-t$. By contrast, if the experiment involves polarized atoms in the presence of an electric field $\boldsymbol{E}$, the observation of a physical signal involving the pseudoscalar $\boldsymbol{E} \cdot \langle \boldsymbol{J} \rangle$ would mean that both P and T are violated. This is just what happens if the atoms are endowed with a static electric dipole moment (EDM). Indeed, it can be shown that T-reversal invariance forbids the existence

of a static electric dipole moment (EDM) for an atomic state if this state is stationary and non-degenerate, i.e. if it has no other degeneracy than that implied by rotational invariance. (In such a case the electric dipole operator restricted to the angular momentum space of the stationary state would necessarily be proportional to the angular momentum operator $\boldsymbol{J}$ which is incompatible with T invariance.)

On the other hand, time-reversal invariance does not forbid the existence of an electric dipole moment of transition between states of the same parity, such as for instance the $n\mathrm{S}_{1/2}$ states of caesium,

$$E_1^{\mathrm{pv}}(n'n) = \langle n'\tilde{\mathrm{S}}_{1/2}m_{\mathrm{s}}|d_z|n\tilde{\mathrm{S}}_{1/2}m_{\mathrm{s}}\rangle$$

where the tilde means that the states are perturbed by the parity-violating part of the Hamiltonian H_{PV} and m_{s} is simply the eigenvalue of J_z. The parity selection rule permits a magnetic dipole of transition between the same two states

$$M_1(n'n) = \langle n'\mathrm{S}_{1/2}m_{\mathrm{s}}|\mu_z/c|n\mathrm{S}_{1/2}m_{\mathrm{s}}\rangle$$

where μ_z is the magnetic moment operator. One more important property follows from T invariance: namely that the ratio E_1^{pv}/M_1 is purely imaginary (for a detailed proof see Bouchiat and Bouchiat (1974a, p 907)). With the usual phase convention M_1 is real so E_1^{pv} is purely imaginary. Note that if $n = n'$ we recover the previously quoted result concerning the EDM, since the diagonal matrix element of an Hermitian operator is necessarily real.

All the atomic PNC effects reported so far are manifestations of *transition dipoles* which violate the parity selection rule, referred to by the spectroscopists as the Laporte rule.

1.5. Parity violation in stable atoms and in nuclear physics: different physical origins and different orders of magnitude

In contrast with Mrs Wu's experiment, the A_{LR} measured in all atomic physics experiments is very small, typically 6×10^{-6}. Sometimes people ask what is the point of performing such a PNC experiment 40 years after Mrs Wu and under more difficult conditions? To make the comparison easier, we can replace the β decay involved in Mrs Wu's experiment by a closely connected process, the capture of an electron in the K shell by a proton of the nucleus. The electron is transformed into a neutrino while the proton is turned into a neutron. The agent responsible for this exchange of electric charge is the weak vector boson $\mathrm{W}^{\pm}$. As we previously explained, in an atomic transition, the nucleus is not modified and the electrons remain electrons. Instead, the symmetry is broken by the exchange of a Z^0 boson, the neutral partner of the $\mathrm{W}^{\pm}$.

In Mrs Wu's experiment, the left–right asymmetry, A_{LR}, results from an interference taking place between the part of the $\mathrm{W}^{\pm}$ exchange amplitude which conserves parity (the P-even component) and that which does not (P-odd). Both parts are of the same order of magnitude and so this leads to a large signal.

The situation is very different in experiments on caesium: the electromagnetic amplitude, A_{em}, which is P-even, dominates the P-odd weak amplitude, A_{W}, (the P-even weak amplitude plays a negligible role.) To first order the atomic left–right asymmetry is twice the real part of $A_{\mathrm{W}}/A_{\mathrm{em}}$ (see section 2.3). Thus it is expected to be small, even for the particular transitions (e.g. $6\mathrm{S} \rightarrow 7\mathrm{S}$ in Cs), which have been chosen for their unusually small A_{em}. It should be clear that although atomic PV measurements are much harder to perform than nuclear beta decay or muon decay experiments, they explore a new domain of electroweak physics.

In particle physics the weak interactions mediated by the electrically neutral Z^0 are called weak neutral current interactions, in contrast with the charged-current interactions

mediated by the charged bosons, W^+ or W^-. The physical information extracted from the study of weak currents turns out to be very different in the two cases. In fact the discovery of neutral current processes in high-energy neutrino scattering on nuclei by the Gargamelle collaboration at CERN (Hasert *et al* 1973) opened up a whole new field in particle physics.

1.6. Main questions addressed in this review

One of the ultimate goals of present experiments on atomic PNC is a precise measurement of the weak charge Q_W, in particular in the case of atomic caesium, a metrological atom *par excellence*. One should, however, bear in mind that a one per cent determination of Q_W requires a precision of 10^{-13} in the measurement of a transition electric dipole, expressed in atomic units. Moreover, other questions merit further consideration: can the experiment tell us if the weak charge is carried out by protons or mainly by neutrons? Can one observe a chiral electron–nuclear potential depending upon the nuclear spin which is expected to arise from a chiral component of nuclear magnetization induced by the electroweak interaction inside the nuclear matter? An answer to this last question has been provided only very recently.

For the last 20 years, the study of electroweak interactions has represented a very important part of the experimental activity in particle physics. It started in 1973 with the discovery at CERN of the 'neutral currents' (Hasert *et al* 1973) processes in neutrino–nucleus scattering and culminated in the discovery of the weak vector bosons $W^{\pm}$ and Z^0 with the CERN proton–antiproton collider (Arnison *et al* 1983a, b, Banner *et al* 1983). The very important experimental programs achieved with the CERN electron–positron collider LEP have led to detailed and precise tests of the electroweak theory (e.g., Rubbia *et al* 1994). Another important milestone was the discovery in 1978 of a left–right asymmetry in a deep inelastic electron–deuteron scattering experiment performed in Stanford (Prescott *et al* 1978, 1979). This provided the first empirical evidence for a chiral electron–quark interaction. In the light of this work, it is then clearly legitimate to ask to what extent atomic experiments can provide valuable information about the electroweak theory? In this review paper we shall do our best to answer to this question.

We begin this review (section 2) by presenting the main features of the electron–nucleus PV interaction resulting from electroweak unification. Their detailed understanding appears as a prerequisite which cannot be circumvented if one wants to succeed in detecting parity violation in atoms. The smallness of the effects to be observed, the fact that they increase faster than Z^3 have led the experimentalists to choose unusual working conditions, as for instance highly forbidden transitions in heavy atoms with oscillator strengths of 10^{-15}. In section 3 we describe both optical rotation measurements in vapours of heavy atoms and Stark experiments in highly forbidden M_1 transitions such as the $6S_{1/2} \rightarrow 7S_{1/2}$ transition in caesium where they have met with undisputable success. In section 4 we review the atomic calculations required to extract from the experimental measurement the weak charge of caesium, the heaviest stable atom with the simplest atomic structure. Atomic theorists have achieved a real *tour de force* to bring the precision of their calculation to the one per cent level. We then discuss several kinds of implications of the results for electroweak theory. It is remarkable that such low-energy measurements have something to add to high-energy particle physics experiments performed near the large accelerators. Furthermore, the most precise measurements in caesium performed on two hyperfine lines obtained, recently, a PV manifestation of a totally new kind: it is sensitive to the nuclear spin-dependent weak interactions taking place inside the nucleus and described in terms of the nuclear anapole moment. Now, there are still various important goals which remain to be reached

(section 5), for instance the study of the variation of the neutron distribution radii along a string of isotopes, so we examine the different kinds of experiments in progress as well as encouraging proposals. In a general way, they resort to non-traditional experimental approaches. This is a good sign, illustrating the current vitality of the field.

Since the work of Pasteur, we know that biological molecules exhibit a chiral behaviour at a much higher level than that observed in inert matter atoms. The suggestion has been made many times (Kondepudi and Nelson 1985, Hegstrom and Kondepudi 1990) that the two phenomena could be connected, despite the tremendous difference in the sizes of the effects involved. The connection has not been established in a totally convincing way and the subject is still open to controversy (Avetisov *et al* 1991); it will not be discussed any further in the present review. We shall limit ourselves to present both the theoretical and experimental problems raised by degeneracy lifting between the two enantiomers of a chiral molecule (see section 2.5) and we shall say a few words about present lines of attack (section 5.5).

2. Possible manifestations of parity violation in atomic and molecular physics

In this section we wish to present the different kinds of experiments performed first to demonstrate and then to measure precisely PNC in atomic transitions. We recall the basic ideas which have oriented the choice of two different experimental approaches, optical rotation measurements and Stark experiments on M_1 forbidden transitions. We describe experiments of both kinds and list the results in tables 1 and 2 in section 3.

2.1. Different PNC tests

As mentioned in the introduction there are different ways to test PNC in a physical process. Even though, as we shall show here, the principles involved in each case are equivalent there are considerable differences as regards the experimental conditions required.

We consider a system governed by a Hamiltonian which contains two parts, one even the other odd under space reflection:

$$H = H^{\text{even}} + H^{\text{odd}}. \tag{1}$$

As a direct result, under the action of the operator P, H transforms as: $P^{-1}HP = H^{\text{even}} - H^{\text{odd}} \neq H$, hence:

$$[P, H] \neq 0. \tag{2}$$

As a first consequence we obtain the non-commutation of H with the parity operator and therefore the non-conservation of the parity quantum number between an initial and a final state:

$$\prod \epsilon_{\text{i}} \neq \prod \epsilon_{\text{f}}. \tag{3}$$

It is easily shown that non-commutation also applies to the time evolution operator, $U(t) = \exp(-\text{i}Ht/\hbar)$:

$$[P, U(t)] \neq 0. \tag{4}$$

If a system is prepared in an initial state which is an eigenstate of P, after a time t it no longer remains in an eigenstate. Let us now compare a transition rate between two

states $P_{A\to B} = |\langle B|U(t)|A\rangle|^2$ to the transition rate between their mirror states, $|\tilde{A}\rangle = P|A\rangle$, $|\tilde{B}\rangle = P|B\rangle$:

$$P_{\tilde{A}\to\tilde{B}} = |\langle\tilde{B}|U(t)|\tilde{A}\rangle|^2 = |\langle B|P^{-1}U(t)P|A\rangle|^2 \neq |\langle B|U(t)|A\rangle|^2. \tag{5}$$

Hence we see that another consequence of PNC is the existence of a difference between the rates of transition between two states and their mirror states

$$P_{A\to B} \neq P_{\tilde{A}\to\tilde{B}}. \tag{6}$$

Yet another consequence arises in connection with the energies of enantiomer molecules

$$E_A = \langle A|H|A\rangle \tag{7}$$

$$E_{\tilde{A}} = \langle A|P^\dagger H P|A\rangle \neq \langle A|H|A\rangle. \tag{8}$$

Hence the energies of two enantiomer molecules are not identical.

As we shall see all these different tests form the bases of different kinds of PNC experiments.

2.2. Coulomb versus electroweak electron–nucleus potential

It is instructive to compare the electron–nucleus potentials describing respectively the Coulomb interaction and the PNC interaction associated with Z^0 boson exchange. In the vicinity of the nucleus the Coulomb potential may be expressed as

$$V_{\text{Coulomb}}(r_e) = \frac{Ze^2}{r_e} \tag{9}$$

where Z is the atomic number while the PNC potential can be written in the non-relativistic limit as:

$$V_{\text{pv}}(r_e) = \frac{1}{2} Q_W g_{Z_0}^2 \frac{\exp(-M_{Z_0} c r_e/\hbar)}{r_e} \boldsymbol{\sigma}_e \cdot \boldsymbol{v}_e/c + \text{HC} \tag{10}$$

where g_{Z_0} is a coupling constant whose size, as a consequence of electroweak unification, is of the order of e. The interest of (9) and (10) lies in the fact that they illustrate the close analogy existing between Ze^2 and $Q_W g_{Z_0}^2$ which represent respectively the strength of the Coulomb and electroweak interactions between the electron and the nucleus. The Z^0 Compton wavelength $\hbar/(M_{Z_0}c)$ is much smaller than the atomic scale characterized by the Bohr radius $a_0 = \hbar/(m_e c\alpha)$ ($\alpha = 1/137$ is the fine structure constant) so that it is legitimate to take the limit of infinite Z^0 mass. The Yukawa potential appearing in (10) can then be replaced by a Dirac distribution

$$\lim_{M_{Z_0}\to\infty} \left(\frac{M_{Z_0}c}{\hbar}\right)^2 \frac{\exp(-M_{Z_0} c r_e/\hbar)}{r_e} = \delta^3(\boldsymbol{r}_e).$$

It is convenient to introduce the Fermi constant G_F which is proportional to $(g_{Z_0}/M_{Z_0})^2$. The standard electroweak theory gives a well defined value for the proportionality coefficient. To have an idea of the scale of the electroweak effect in atoms it is instructive to write the values of G_F in atomic units

$$G_F = 4 \times 10^{-14}\ \text{Ryd} \times a_0^3.$$

We can now write the expression of the potential $V_{\text{pv}}(r_e)$ in the form usually found in the literature

$$V_{\text{pv}}(r_e) = \frac{Q_W G_F}{4\sqrt{2}} (\delta^3(\boldsymbol{r}_e)\boldsymbol{\sigma}_e \cdot \boldsymbol{v}_e/c + \text{HC}). \tag{11}$$

Like the nuclear electric charge Z, the weak charge Q_W is the sum of the weak charges of all the constituents of the atomic nucleus, the u and d quarks

$$Q_W = (2Z + N)Q_W(u) + (Z + 2N)Q_W(d). \tag{12}$$

In the standard model it so happens that Q_W lies close to the neutron number†

$$Q_W(SM) = -N - Z(4\sin^2\theta_W - 1) \simeq -N \tag{13}$$

where the weak mixing angle θ_W is a free parameter of the theory, given experimentally by $\sin^2\theta_W = 0.23$.

One should also note that for distances smaller than the Z^0 Compton wavelength the ratio $V_{pv}(r_e)/V_{Coulomb}(r_e)$ is given, to within the helicity factor $\boldsymbol{\sigma}_e \cdot \boldsymbol{v}_e/c$, by the quantity $(Q_W/Z) \times (g_{Z_0}^2/e^2)$ which is of order unity. This shows clearly that the smallness of the electroweak effects in atoms follows solely from the fact that the range of the potential $V_{pv}(r_e)$ is exceedingly small compared to typical atomic sizes, roughly by a factor 2×10^7.

Behind the obvious similarity between the electric and weak charge of the nucleus lie hidden significant differences. These are already visible in (13). The ratio of the electric charges of two arbitrary nuclei is a rational number. This is not so for the corresponding weak charge ratio since $\sin^2\theta_W$ is not in general a rational number, unless the electroweak gauge group is embedded in a larger semi-simple group; but even in that case, electroweak higher-order effects would spoil this property. Furthermore, the additivity rule, shown explicitly in (12), is valid strictly only to lowest order in the electroweak interaction. This is due to the fact that the Z_0 current conservation is broken by higher-order electroweak effects. However, it should be stressed that, in practice, corrections to (12) remain below the 1% level.

2.3. The difficulty of detecting electroweak processes in atoms

The first question which arises when one begins to think about electroweak processes in atoms is of course their order of magnitude. For a naive order of magnitude estimate one can consider two different electron–hadron radiative processes. One, of amplitude A_{em}, is exclusively governed by electromagnetic processes while the second, of amplitude A_W, involves a Z^0 exchange. The weak amplitude is expected to contain a contribution odd under space reflection which can give rise to a left–right asymmetry A_{LR} by interference with the dominant electromagnetic amplitude. With $P_{L/R} = |A_{em} \pm A_W^{odd}|^2$ we find

$$A_{LR} = \frac{P_L - P_R}{P_L + P_R} = 2\,\mathrm{Re}(A_W^{odd}/A_{em}). \tag{14}$$

If q denotes the four-momentum transfer between the lepton and the hadron, A_{em} is proportional to e^2/q^2 while $A_W \propto g^2/(q^2 + M_{Z_0}^2c^2)$. In atoms we expect q to be given by the inverse of the Bohr radius $q \sim \hbar/m_e\alpha c$. For the left–right asymmetry we thus arrive at an exceedingly small value

$$A_{LR} \simeq \alpha^2 \frac{m_e^2}{M_{Z_0}^2} \approx 10^{-15}.$$

Such a result would appear to make the observation of the left–right asymmetry completely hopeless. Indeed, this was the conclusion reached very early on by Zel'dovich (1959), who raised the question of the existence of parity violation in atoms much before the advent of unified gauge theories. He gave the first discussion of the possible effects in atomic

† As specified below, formula (13) is valid only to lowest order in the electroweak interaction.

physics of a weak electron–nucleon interaction induced by so-called neutral currents. In particular, he estimated the rotation of the plane of polarization of visible light propagating through optically inactive matter to be of the order of 10^{-13} rad m^{-1} and concluded that obviously such an effect would be unobservable. Except for the possibilities reexamined by Curtis-Michel (1965) which were also not very promising, the subject remained at a complete standstill until the active search for neutral currents in particle physics started in the early 1970s.

It is at that time that the authors became strongly motivated to take a new look at this problem for two reasons. First, because of the rapid developments taking place in weak interaction field theory, the problem of the existence of weak neutral currents was taking on a new dimension. After a certain period of an active search for neutral currents with neutrino beams, with no success, theorists started to develop models in which neutral currents *existed only with charged leptons* (Prentki and Zumino 1972, Lee 1972). In such a case atomic physics measurements seemed an obvious testing ground. The second reason was the revolutionary advances taking place in laser technology with the apparition of highly monochromatic tunable laser sources would make such experiments feasible.

Of course if the above orders of magnitude had turned out to be true we would not be discussing the subject here today. In fact, the above naive estimate is far too pessimistic for left–right asymmetries in atomic physics where values as large as a few times 10^{-6} and up to 10^{-5} have actually been observed (several reviews cover these topics, Commins 1981, Bouchiat and Pottier 1986, Commins 1987, Stacey 1992). This difference is explained by the existence of enhancement mechanisms.

2.4. Enhancement mechanisms

2.4.1. The Z^3 law. In 1974 we predicted that the electroweak effects in atoms should grow a little faster than the cube of the atomic number Z (Bouchiat and Bouchiat 1974a,b). As one might expect, this Z^3 law has had a strong impact upon the experimental programs over the last 20 years. The weak charge $Q_W \simeq -N$ accounts for the first Z factor since the ratio N/Z is $\geqslant 1$ for most complex stable nuclei. The second factor Z reflects the well known fact that in the vicinity of the nucleus the electronic density of penetrating valence orbitals grows like Z. The third Z factor can be traced back to the helicity factor $\boldsymbol{\sigma}_e \cdot \boldsymbol{v}_e/c$ appearing in $V_{pv}(r_e)$. Near the nucleus the electronic orbital is nearly Coulombic and as a consequence, the electronic velocity $\boldsymbol{v}_e$ is proportional to the nuclear charge Z.

In our 1974 paper, we gave, of course, a precise analytical justification of the above hand-waving arguments, based on the independent particle model of the atom. Our derivation is valid for any realistic one-electron self-consistent local potential. As a starting point, we use the following representation of the radial electronic wavefunction of an arbitrary angular momentum state

$$R_{nl}(r) = \frac{1}{r} C_{nl} \sqrt{\frac{\phi(r)}{\phi'(r)}}\, J_{2l+1}(\sqrt{8\phi(r)}). \tag{15}$$

The function $\phi(r)$ obeys a nonlinear equation, similar to that used to get a high-order JWKB approximation, except that in the present problem the quantity playing the role of $\hbar$ turns out to be $Z^{-1/3}$. Near the origin the function $\phi(r)$ can be computed exactly. It reduces to Zr/a_0, to within a well defined correction factor of order unity, when $l \geqslant 1$. The main problem was then to compute the normalization constant C_{nl}. This has been achieved, up to the order $Z^{-4/3}$, by matching the wavefunction of (15) with the large r limit asymptotic wavefunction given by quantum defect theory. For heavy atoms the constant C_{nl} turns out to

be independent of Z, a non-trivial result. (For hydrogenic atoms $C_{\rm nl}$ is instead proportional to Z.)

We thus obtained, in atomic units,

$$\lim_{r\to 0}(R_{\rm nl}(r)/r^l) = \frac{(2Z)^{l+1/2}}{(2l+1)!}({\rm d}n/{\rm d}\epsilon)^{-1/2}(1+\delta_l).$$

The level density ${\rm d}n/{\rm d}\epsilon$ is close to unity for valence states and the correction term δ_l is shown to be negligible in heavy atoms. The Z^3 law is then readily deduced by computing the matrix element of the potential $V_{\rm pv}(r_{\rm e})$ given by (11),

$$\langle n{\rm s}_{1/2}|V_{\rm pv}|n'{\rm p}_{1/2}\rangle = \frac{3{\rm i}}{16\pi m_{\rm e}}\frac{G_{\rm F}}{\sqrt{2}}Q_{\rm W}\lim_{r\to 0}(R_{n{\rm s}_{1/2}}(r)R_{n'{\rm p}_{1/2}}(r)/r)$$

using the wavefunctions and the results indicated above.

For heavy atoms relativistic effects are significant, especially in the vicinity of the nucleus. We computed the correction factor to be applied to the above formula that we rewrite here in an approximate form

$$K_r \approx (a_0/2ZR_{\rm W})^{Z^2\alpha^2}. \tag{16}$$

The correction factor K_r gives rise to a further increase with Z. The factor K_r reaches a value of 2.8 for Cs and 9 for Bi, Pb and Tl (Bouchiat and Bouchiat 1974b). In K_r we can note the presence of the radius $R_{\rm W}$ of the weak charge of the nucleus. Since, as a result of a numerical accident making $(1-4\sin^2\theta_{\rm W})\simeq 0$ the weak charge is carried essentially by the neutrons, precise PV measurements should give unique information on the neutron distribution, assuming the standard model is valid (see section 5).

2.4.2. PNC and EDM in heavy atoms. An analogy has been suggested between the Z^3 law in atomic parity violation and the 'anti-screening' of the electron EDM in heavy atoms (Sandars 1987). We would like to note that such an analogy is somewhat superficial and does not go much beyond the observation that both effects are increasing functions of Z.

The Z^3 law in atomic parity violation was first derived in a *non-relativistic* one-particle model of the atom (Bouchiat and Bouchiat 1974b). The physical origins of three contributions, each one proportional to Z have just been given (section 2.4.1). By contrast the 'anti-screening' of the electron EDM is a *truly relativistic* atomic effect; the electron EDM is completely screened in atoms described by the Schrödinger equation. In the Dirac theory the atomic EDM can be incorporated (Sanders 1987) by adding to the Hamiltonian the P and T violating term $2{\rm i}\beta\gamma_5\boldsymbol{p}^2 d_{\rm e}$ *which is cubic in the electron velocity* and bears little resemblance to the electron–nucleus PV potential. We have just seen that relativistic effects also modify the PV potential matrix element, leading to the peculiar non-analytic correction factor K_r (16). This latter reflects, on the one hand, the zero range nature of the PV electron–nucleon interaction and on the other, the singular behaviour of the Coulomb–Dirac wavefunction near the origin. No such singular dependence upon the nuclear radius is apparently present in the anti-screening effect.

From the above considerations, it follows that the physical mechanisms behind the Z increase are different in atomic parity violation and in anti-screening of the electron EDM in heavy atoms.

2.4.3. Excitation of highly forbidden transitions. The second enhancement mechanism comes from the excitation of highly forbidden atomic transitions like the $6{\rm S}_{1/2}$–$7{\rm S}_{1/2}$

transition in atomic caesium (Bouchiat and Bouchiat 1974a). This atom, even today, still appears the best compromise between a high value of Z and the simplicity of the atomic structure which helps one to perform reliable atomic physics calculations.

QED strictly forbids the existence of an electric dipole amplitude between two atomic states having the same parity. The Z^0 exchange interaction breaks this rule and gives rise to a small but non-zero electric dipole amplitude $E_1^{\rm pv}$ which can reveal its presence in atomic physics, $E_1^{\rm pv} \simeq {\rm i} \times 10^{-11} e a_0$. A magnetic dipole amplitude is allowed by symmetry, but because the two states involved have different radial quantum numbers, it is very much reduced, $M_1 \simeq 0.4 \times 10^{-4} \mu_{\rm B}/c$. Consequently the asymmetry may be expected to reach a rather large value, $A_{\rm LR} = 2\,{\rm Im}(E_1^{\rm pv}/M_1) \approx 10^{-4}$.

In practice, however, the transition is so suppressed (oscillator strength 4.0×10^{-15}) that at the atomic densities required to see a signal, it is masked by a background coming from weakly bound molecules. We proposed a solution to this problem by introducing a static electric field $\boldsymbol{E}$. In this case the Stark effect is responsible for an E_1 Stark-induced amplitude proportional to E (Bouchiat and Bouchiat 1975). The degree of forbiddenness of the transition is controlled by adjusting the strength of the field. In actual experiments the asymmetry, $2\,{\rm Im}\,(E_1^{\rm pv}/E_1^{\rm stark})$, turns out to be a few times 10^{-6} or even 10^{-5}. We can note that increasing the electric field increases the transition rate proportionally to E^2 while it decreases the asymmetry as $1/E$.

2.4.4. Accidental degeneracy between two opposite parity states. Finally, as a third possibility of enhancement there is the accidental degeneracy which can occur between an S and a P state. In the parity mixing coefficient $\langle n{\rm s}_{1/2}|V_{\rm pv}|n'{\rm p}_{1/2}\rangle/(E_{n{\rm s}_{1/2}} - E_{n'{\rm p}_{1/2}})$, the small energy denominator nearly compensates for the lack of Z^3 enhancement. This is the case for the metastable $2{\rm S}_{1/2}$ state in atomic hydrogen. Unfortunately, in real experiments there are serious problems with stray electric fields. Indeed, the same degeneracy which reinforces $E_1^{\rm pv}$, also reinforces the Stark-induced amplitudes.

In spite of strong difficulties Williams and collaborators at Michigan University enthusiastically devised a beautiful experiment with hydrogen (Levy and Williams 1982) which, most unfortunately, he was unable to complete before his passing away in an accident. Two other experiments in Seattle (Adelberger *et al* 1981) and at Yale (Hinds 1980, 1988) met with insurmountable difficulties.

Nevertheless, this third enhancement mechanism does lead to better prospects if it can be cumulated with the Z^3 enhancement which is free from the same drawback. An exceptional situation in dysprosium has been pointed out by the Novosibirsk group (Dzuba *et al* 1986) and is currently being investigated by the Berkeley group who have joined forces by Budker and Zolotorev from Novosibirsk (see section 5.2.1 and Budker *et al* 1983). Another interesting case also seems to exist in samarium (see section 5.2.2). However, it must be emphasized that quasi-degeneracy is not sufficient to produce a large enhancement of the PV effect; the quasi-degenerate levels must have the same electronic angular momentum and opposite parities to be connected by $V_{\rm pv}$, but in addition they must also correspond to a configuration where a ${\rm p}_{1/2}$ electron is substituted for an ${\rm s}_{1/2}$ electron, at least in a substantial proportion when configuration mixings occur. In complicated atomic structures such as those of rare earths it is this last condition which is the most difficult to achieve or even to verify. More precisely the spectroscopic information required to test whether it really holds is often unavailable. Moreover, the number of states contributing to parity mixing does not necessarily reduce to just the closest one, and in the summation required to predict an effect important cancellations may occur.

2.5. Energy shifts due to parity-violating electron–nucleus interaction in chiral molecules

The measurement of the energy difference between the mirror images of a chiral molecule has a twofold interest. First it would be the first manifestation of PV atomic forces in a static situation while all the effects discussed in this review refer to transition processes. Second, the magnitude of this energy difference is important for physicists who are looking for a connection between the electroweak interaction and the chiral behaviour of biological molecules (Letokhov 1975, Kondepudi and Nelson 1985, Hegstrom and Kondepudi 1990, Avetisov *et al* 1991, Mason 1984).

In this section we shall not analyse in detail the explicit computations which have appeared in the literature (see for instance Rein *et al* 1979, Hegstrom *et al* 1989). A review of the state of the art in this difficult subject is beyond the competence of the authors. We shall rather illustrate with simple models the physical problems one encounters in such an evaluation. It is also instructive to analyse the formal analogy between the PV energy shift and the optical rotation of chiral molecules.

2.5.1. Order of magnitude and Z^5-dependence. The first important property of the PV energy shift $\Delta E_{\rm PV}$, first noted by Gajzago and Marx (1974) follows from T invariance. If the spin–orbit coupling is neglected, more generally in the absence of any spin-dependent interaction, $\Delta E_{\rm PV}$ vanishes for an arbitrary molecular stationary state $|\Psi^n\rangle$. Indeed, in the LS coupling limit, the wavefunction can be factorized as

$$\Psi^n(\boldsymbol{r}_1, \sigma_1, \ldots, \boldsymbol{r}_n, \sigma_n) = \chi_{S,M_S}(\sigma_1, \ldots, \sigma_n)\Phi^n(\boldsymbol{r}_1, \ldots, \boldsymbol{r}_n).$$

Time-reversal invariance is equivalent here to complex conjugation of the spatial wavefunction. As a consequence, the wavefunction Φ^n can always be taken to be real, as is usually done in molecular physics computations. The energy shift induced by the electron–nucleus PV potential can be written in the LS coupling scheme as

$$\begin{aligned}\Delta E^n_{\rm PV} &= \langle\Psi^n| \sum_{ik} V_{\rm pv}(\boldsymbol{r}_{ik})|\Psi^n\rangle \\ &= \frac{G_{\rm F}}{2\sqrt{2}} M_{\rm S} \sum_k Q^k_{\rm W}\, {\rm Re}(\langle\Phi^n|\delta^3(\boldsymbol{r}_{1k})\, p_{z_1}|\Phi^n\rangle)\end{aligned} \tag{17}$$

where i indexes the electrons and k the nuclei. The function Φ^n being real, the above expression vanishes since p_{z_1} is a purely imaginary operator. In fact, in order to get a finite quantity it is necessary to include the spin–orbit correction at least to first order.

An evaluation of the matrix element of $V_{\rm pv}$ carried out by the authors (Bouchiat and Bouchiat 1974b) and a textbook formula for the spin–orbit splittings, lead to the following estimates in the high-Z limit:

$$\begin{aligned}\langle {\rm s}_{1/2}|V_{\rm pv}|{\rm p}_{1/2}\rangle &\simeq -{\rm i}\frac{Q_{\rm W}G_{\rm F}m_{\rm e}^2}{2\pi\sqrt{2}}(Z\alpha)^2(\nu_s\nu_p)^{-3/2}K_r\ {\rm Ryd} \\ \langle {\rm p}_{1/2}|V_{\rm so}|{\rm p}_{1/2}\rangle &\simeq -\tfrac{1}{3}(Z\alpha)^2\nu_p^{-3}H_r\ {\rm Ryd}\end{aligned}$$

where ν_s and ν_p are, respectively, the effective radial quantum numbers for the ${\rm s}_{1/2}$ and ${\rm p}_{1/2}$ single-particle states; K_r and H_r are known relativistic correction factors which can be appreciably larger than unity. From the above equations one can derive a crude estimate for $|\Delta E_{\rm PV}|$ which has to be considered as an upper bound, as will become clearer below

$$|\Delta E_{\rm PV}| \sim \frac{Q_{\rm W}G_{\rm F}m_{\rm e}^2}{3\pi\sqrt{2}}(Z\alpha)^4 H_r K_r Ry \sim 10^{-21}Z^5 K_r\ {\rm Ryd} \tag{18}$$

where, for simplicity, we have dropped the dependence on the effective radial quantum numbers.

2.5.2. Similarities and differences with optical rotation. The Z^5 dependence of $\Delta E_{\rm PV}$, compared to Z^3 with atoms makes it even more imperative to work with a molecule which contains heavy nuclei. We shall assume, from now on, that there is just a single heavy nucleus in the molecule so that we can limit ourselves to the contribution to $\Delta E_{\rm PV}$ associated with molecular orbitals $\Phi^n(\boldsymbol{r})$ centred on the heavy nucleus, taken as the origin of the electron coordinate. After some simple manipulations involving the spin operator, we obtain the *single-particle* expression to lowest order in spin–orbit correction

$$\Delta E^n_{\rm PV}({\rm s.p.}) = \frac{G_{\rm F}Q_{\rm W}}{4\sqrt{2}}\,{\rm Re}(\langle\Phi^n|\delta^3(\boldsymbol{r})\boldsymbol{p}G(E_n)\cdot\boldsymbol{L}\xi(r)|\Phi^n\rangle). \tag{19}$$

In the above equation, the spin–orbit potential $\xi(r)\boldsymbol{L}\cdot\boldsymbol{s}$ is associated with the screened Coulomb potential of the heavy nucleus and $G(E)$ is the Green function of the single-particle Hamiltonian $H_{\rm mol}$ associated with the molecular orbitals $\Phi^n(\boldsymbol{r})$.

As was pointed out by Rein *et al* (1979), it is instructive to compare the above expression of $\Delta E_{\rm PV}$ with the one giving the optical rotation of the molecule $R(\omega)$, within the same single-particle model. To make the comparison easier we have rewritten the usual textbook formula giving optical rotation in terms of the dipole velocity operator. To within a constant, the optical rotation can be expressed as

$$R(\omega) \propto {\rm Re}(\langle\Phi^n|\boldsymbol{p}(G(E_n+\hbar\omega)+G(E_n-\hbar\omega)-2G(E_n))\cdot\boldsymbol{L}|\Phi^n\rangle). \tag{20}$$

As far as spatial symmetry considerations are concerned, the similarity between the expressions giving $R(\omega)$ and $\Delta E^n_{\rm PV}$(s.p.) is obvious. We note, however, a very important difference. In $\Delta E^n_{\rm PV}$ the operators $\boldsymbol{p}$ and $\boldsymbol{L}$ appear multiplied by $\delta^3(\boldsymbol{r})$ and $\xi(r)$ which both have a short-range feature. This means that $\Delta E^n_{\rm PV}$ will receive its main contribution from the molecular wavefunction in the vicinity of the nucleus, while $R(\omega)$ will depend mostly on the wavefunction outside the atomic core. As a consequence, $R(\omega)$ is likely to be more sensitive than $\Delta E^n_{\rm PV}$ to the lack of mirror symmetry of the molecular wavefunction.

2.5.3. The single-centre theorem. In order to get some insight into the problem, we shall first consider an s–p orbital $\Phi^n(\boldsymbol{r})$ written in Cartesian form as

$$\Phi^n(\boldsymbol{r}) = a^n(r) + \boldsymbol{b}^n(r)\cdot\boldsymbol{r} \tag{21}$$

where $a^n(r)$ and $\boldsymbol{b}^n(r)$ are real functions of the radial electron coordinate r. In the spirit of the Born–Oppenheimer approximation, they are also functions of the coordinates $\boldsymbol{R}_k$ of the other nuclei. In practice, the molecular states are often invariant upon simultaneous rotations of the electrons and nuclei, at least statistically, so that $\boldsymbol{b}^n(r)$ can be written as

$$\boldsymbol{b}^n(r,\boldsymbol{R}_k) = \sum_k \beta^n_k(r,R_k)\boldsymbol{R}_k. \tag{22}$$

Let us now compute $\Delta E^n_{\rm PV}$ using our *ansatz* for the molecular orbital

$$\Delta E^n_{\rm PV}({\rm s.p.}) = \frac{G_{\rm F}Q_{\rm W}}{3\sqrt{2}}\sum_{n'\neq n}(E_n-E_{n'})^{-1} \times\int {\rm d}^3r(a^n(0)\boldsymbol{b}^{n'}(0)-a^{n'}(0)\boldsymbol{b}^n(0))\cdot(\boldsymbol{b}^{n'}(r)\wedge\boldsymbol{b}^n(r))r^2\xi(r). \tag{23}$$

If the number of different 'light' nuclei is smaller than three the above expression vanishes, as expected. Note also that in order to prevent the possibility of a finite inversion probability,

whereby one of the enantiomers gets transformed into its mirror-image the number of 'light' nuclei should be at least equal to four.

If the p component $\boldsymbol{b}^{n'}(r)\cdot\boldsymbol{r}$ of the orbital $\Phi^{n'}(\boldsymbol{r})$ is a linear combination of p atomic orbitals having the same radial quantum number, the vectors $\boldsymbol{b}^{n'}(r)$ are then collinear for all values of r and, as a consequence, the above equation leads to a null result for the PV energy shift. We note that the result just derived is just a simplified version of the so-called single-centre theorem (Hegstrom *et al* 1989).

Under the influence of the interaction with the other atoms of the molecule, however, the p orbitals become distorted and the vector $\boldsymbol{b}^{n'}(r)$ is actually a linear superposition of atomic p orbitals with different quantum numbers: $\boldsymbol{b}^{n}(r)=\sum_{n_1}\boldsymbol{C}_{nn_1}F_{1n_1}(r)$, where $F_{1n_1}(r)\propto R_{1n_1}(r)/r$, with the normalization condition: $F_{1n_1}(0)=1$. For the values of r relevant here for the evaluation of the spin–orbit splittings, ($r\leqslant a_0/Z$), the function $F_{1n_1}(r)$ varies slowly with the radial quantum number n_1, as can be verified by studying the fluctuations with n_1 of the ratio of the spin–orbit splitting by the square of the p-wave starting coefficient. In conclusion, in spite of the p orbital distortion, a strong suppression of ΔE_{PV} with respect to the standard upper estimate given by formula (18), is still expected in chiral molecules having a single heavy atom, at least within a single-particle model based on hybridized s–p orbitals. An expression similar to (23) can be derived for the optical rotation $R(\omega)$ but the distortion of the p orbitals will play an even larger role since much larger values of r are involved.

A two-centre computation has been performed by Hegstrom *et al* (1989) for twisted ethylene; in this case the 'heavy atoms' are the two carbon atoms. They found a reduction factor of 4×10^{-3} with respect to the standard estimate, due in part to the large amount of cancellation between the various contributing terms.

2.5.4. Molecular s–p–d orbitals with a Coulomb octupole potential. We shall now consider a single-centre model involving hybridized s–p–d orbitals associated with the following single-particle molecular Hamiltonian

$$H_{\mathrm{mol}}=H_{\mathrm{at}}+V_{\mathrm{mol}}(\boldsymbol{r});\ V_{\mathrm{mol}}(\boldsymbol{r})=Az+B_1(x^2-y^2)+B_2(x^2+y^2-2z^2). \tag{24}$$

The above expression for V_{mol} is supposed to be valid for the values of r relevant for the computation of ΔE_{PV} and we assume for the moment that the symmetries of V_{mol} are also valid for larger values of r. Let us write the three orbitals σ, π_x, π_y compatible with the symmetries of H_{mol} as

$$\sigma=a(r)+b_0(r)z\qquad \pi_x=b_1(r)x+d_1(r)xz\qquad \pi_y=b_2(r)y+d_2(r)yz. \tag{25}$$

H_{mol} is invariant under the reflections P_x and P_y with respect to the planes $x=0$ and $y=0$, so ΔE_{PV} vanishes. The simplest way to break the previous symmetries is to add the octupole potential $V_{\mathrm{oct}}=Cxyz$. Under the perturbation of V_{oct} the orbitals are modified as follows: $\sigma\rightarrow\tilde{\sigma}=\sigma+\tilde{d}(r)xy$, $\pi_x\rightarrow\tilde{\pi}_x=\pi_x+\tilde{b}_2(r)y+\tilde{d}_2(r)yz$ and $\pi_y\rightarrow\tilde{\pi}_y=\pi_y+\tilde{b}_1(r)x+\tilde{d}_1(r)xz$. One may remark that the effect of V_{oct} on the π_x, π_y orbitals can be viewed as a small rotation around the z axis, which indicates clearly that chirality has been induced. Note that this effect requires d_{xz}, d_{yz} orbitals to be initially present in π_x, π_y, which means that V_{mol} contains an electric dipole term. The computation of $\Delta E^n_{\mathrm{PV}}(\sigma)$ is straightforward and we have kept only the dominant spin–orbit contribution involving p orbitals

$$\Delta E^n_{\mathrm{PV}}(\sigma)=\frac{G_{\mathrm{F}}Q_{\mathrm{W}}}{9\sqrt{2}m_{\mathrm{e}}}\left[-a(0)\tilde{b}_1(0)\int b_0(r)b_2(r)\xi(r)r^4\,\mathrm{d}r(E_1-E_2)^{-1}+1\leftrightarrow2\right] \tag{26}$$

where E_1, E_2 are respectively the energies of the π_x, π_y states. One can verify that $\Delta E^n_{\mathrm{PV}}(\sigma)$ vanishes if $B_1 = 0$, since in that case H_{mol} is symmetric under the exchange: $x \leftrightarrow y$ i.e. invariant under space reflection with respect to the plane $x - y = 0$. In conclusion, $\Delta E^n_{\mathrm{PV}}(\sigma)$ vanishes if the product $A \times B_1 \times C = 0$ cancels.

It is of some interest to evaluate the optical activity within the same model and more precisely in the case $A = 0$. The Hamiltonian H_{mol} including the electric octupole, but without the electric dipole, is invariant under the group D_2 generated by the three rotations $R_x(\pi)$, $R_y(\pi)$ and $R_z(\pi)$. The orbitals $\tilde{\pi}_x, \tilde{\pi}_y$, belonging to irreducible representations of D_2 reduce to

$$\tilde{\pi}_x = b_1(r)x + \tilde{d}_2(r)yz \qquad \tilde{\pi}_y = b_2(r)y + \tilde{d}_1(r)xz.$$

The optical activity is induced by the mixed $E_1M_1\tilde{\pi}_x \rightarrow \tilde{\pi}_y$ transition. We have computed the optical rotation using the length dipole form and keeping for simplicity only one intermediate state.

$$R(\omega) \propto \int b_1(r)b_2(r)r^4\,\mathrm{d}r \int (b_1(r)\tilde{d}_1(r) + b_2(r)\tilde{d}_2(r))((E_1 - E_2)^2 - (\hbar\omega)^2)^{-2}.$$

In this simple example, we see that optical rotation and the PV shift obey different selection rules since invariance under the D_2 group forbids a PV shift, while optical activity is allowed.

2.5.5. Energy differences in the NMR spectrum of enantiomer molecules. Later on (see section 4.3), we shall discuss the existence of a small contribution to the electron–nucleus interaction ($\sim 10^{-2}$) which depends on the nuclear spin. About ten years ago it was pointed out that the nuclear spin-dependent term can combine with magnetic interactions in a chiral molecule to give nuclear shielding coefficients which depend on the enantiomer (Barra *et al* 1986). Therefore the NMR frequencies of two chiral molecules would be different. Although very small ($\sim 10^{-12}$ in relative magnitude), this energy shift is perhaps measurable (Barra *et al* 1988). It would present the great advantage of providing direct information about the nuclear spin-dependent contribution to the PV interaction.

3. Parity-violation measurements in atomic radiative transitions

Once the Z^3 enhancement became apparent, the main question was how best to take advantage of it.

3.1. Where to search for parity violation in atomic physics

There were in fact two different lines of attack. The first takes advantage of highly forbidden M_1 transitions like $6S_{1/2}$–$7S_{1/2}$ in caesium. Its merits are the relatively large asymmetry and the simple atomic structure characteristic of an alkali atom which has a single electron outside a tight atomic core. This type of transition, however, represented completely new territory and the suppression factor looked absolutely huge, $\sim 10^{14}$, so that one could anticipate difficulties with the signal-to-noise ratio. The latter problem was likely to be tempered by exploiting the effect of a Stark field (see section 2.4.3) but there existed little experimental information concerning this effect for $nS_{1/2}$–$n'S_{1/2}$ transitions and none concerning the low-lying valence states. Nevertheless, this was the approach chosen by our group in Paris. The forbidden M_1 $6P_{1/2}$–$7P_{1/2}$ transition in Tl, also attractive (Bouchiat and Bouchiat 1974b), was selected by the Berkeley group (Neuffer and Commins 1977).

The second line of attack consists in working with allowed M_1 transitions in atoms of even higher Z such as for instance the two well known intercombination lines of bismuth, the infrared line $(6s^2 6p^3)J = 1/2 \rightarrow (6s^2 6p^3)J = 1/2$ at 876 nm and the red line $(6s^2 6p^3)J = 1/2 \rightarrow (6s^2 6p^3)J = 3/2$ at 648 nm. The advantage seemed to be a much lower suppression factor $\sim 10^5$ and *a priori* this should avoid the signal-to-noise difficulties. However, the left–right asymmetry was obviously smaller and the atomic structure quite complicated. In fact Bi often behaves as a trivalent atom and, in certain conditions, a pentavalent one. This approach was adopted by the groups of Oxford, Seattle and Novosibirsk who immediately started experiments (Sandars 1975, Khriplovich 1974) and by the Moscow group somewhat later.

These two lines of investigation have led to experiments of very different kinds: the forbidden transitions were so weak that they were detected by fluorescence while the M_1 allowed transitions could be observed by transmission. In the second case the PNC weak interaction manifests itself via a difference in the index of refraction for right- and left-circularly polarized light. When plane polarized light propagates through the vapour, a rotation of its plane of polarization can be observed near the M_1 transition frequency. The line shape of this rotation follows the dispersive real part of the index of refraction.

3.2. Optical rotation experiments

At first these experiments encountered serious problems with discrimination against systematic effects. The results in Bi varied from one laboratory to another and within the same laboratory at different times. The most recent results from each group are summarized in table 1 which gives both theoretical predictions and the various experimental values. Results exist for the two lines of Bi, in Pb and in Tl (allowed M_1 $6P_{1/2}$–$6P_{3/2}$ transition). The situation now looks much more satisfactory except for the case of the Bi red line; we can note a discrepancy by a factor of 2.2 between the early (unrevised) Novosibirsk result on the one hand and the Oxford and Moscow results on the other. A more recent result from Oxford (-9.8 ± 0.9) has confirmed the previous one with an improved (9%) accuracy (Warrington *et al* 1993). We also remark that there is a large theoretical uncertainty for this particular Bi transition which is due to a strong cancellation of different contributions.

Table 1. Summary of optical rotation results: only the most recently published experimental value of $R = (\mathrm{Im}\, E_1^{\mathrm{pv}}/M_1) \times 10^8$ from each group is presented. Theoretical values are given for $\sin^2\theta_{\mathrm{W}} = 0.230$ and restricted to the most recent work.

	Bi(648 nm)	Pb(1.28 μm)	Bi(876 nm)	Tl(1.28 μm)
Th	-7.5 ± 5[a]	-9.6 ± 0.7[e]	-11.0 ± 1.3[g]	-14.6 ± 0.44[j]
Ex	-9.8 ± 0.9[b]	-9.86 ± 0.12[f]	-10.12 ± 0.20[h]	-15.68 ± 0.45[k]
	-7.8 ± 1.8[c]		-10.4 ± 1.7[i]	-14.68 ± 0.17[l]
	-20.2 ± 2.7[d]			

(a) Dzuba *et al* (1989b); (b) Warrington *et al* (1993); (c) Birich *et al* (1984); (d) Barkov and Zoloterev (1980); (e) Dzuba *et al* (1988); (f) Meekhof *et al* (1993); (g) Dzuba *et al* (1989b); (h) Macpherson *et al* (1991); (i) Hollister *et al* (1981); (j) Dzuba *et al* (1987); (k) Edwards *et al* (1995); (l) Vetter *et al* (1995).

A remarkable experimental accuracy has been obtained in the infrared line of Bi (2%), (Macpherson *et al* 1991, see figure 1) and more recently in thallium (Vetter *et al* 1995). In both cases the fact of performing the measurements at high optical density proved to be essential to reach this high accuracy. Possible sources of systematics were extensively

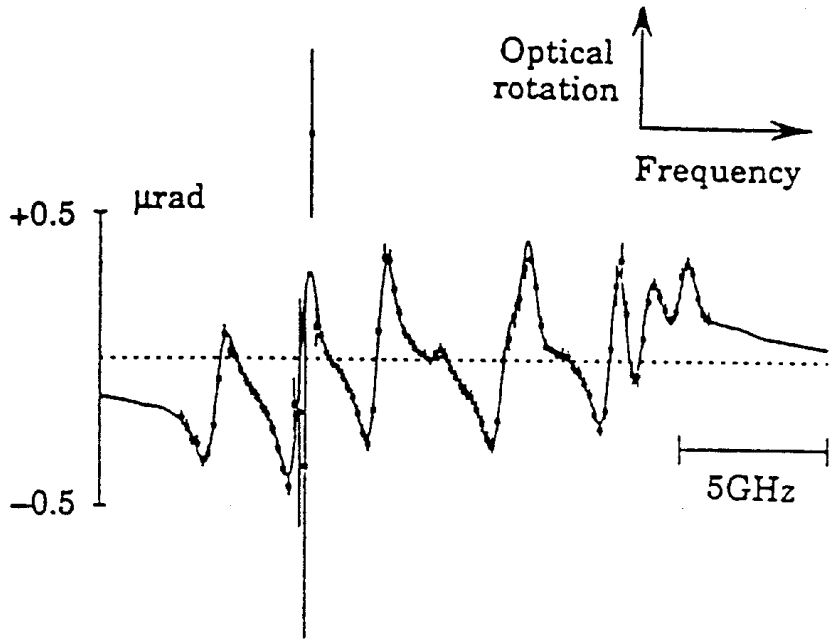

Figure 1. Optical rotation results obtained in Bi at 876 nm (Macpherson *et al* 1991).

studied. Since wavelength dependence is the sole criterion available to distinguish the PNC optical rotation from stray effects, a detailed understanding of the line-shape profile was crucial to the success of the experiments.

Clearly the accuracy of the determination of Q_W in thallium is now limited by the uncertainty (3%) arising from atomic theory.

3.3. Stark experiments in forbidden M_1 transitions of Cs and Tl

In the early seventies there had been practically no experimental and theoretical study concerning the $nS_{1/2} \rightarrow n'S_{1/2}$ transitions in alkali atoms. It turns out that, independently of the parity-violation problem, the physics related to these transitions has its own interest. The various transition amplitudes, to be discussed below, lead to new interference effects, like for instance, a new form of optical pumping, where the angular momentum transferred to the atom is transverse to the light beam direction (formula (28) below). These effects have allowed an empirical determination of the forbidden M_1 amplitude which is practically impossible to measure directly.

In order to discuss electroweak parity violation in highly forbidden transitions it is convenient to introduce an effective dipole operator (Bouchiat and Bouchiat 1975). This is a hybrid vector-type quantity which behaves as a matrix element in the radial atomic coordinate space and as an operator in the spin space; $\boldsymbol{\sigma}$ is the spin operator. It contains the various components which govern the interaction with the radiation field exciting the $nS_{1/2}$–$n'S_{1/2}$ (or $nP_{1/2}$–$n'P_{1/2}$) transition

$$\boldsymbol{d}_{\text{eff}} = -\alpha(n', n)\boldsymbol{E}_0 - \mathrm{i}\beta(n', n)\boldsymbol{\sigma} \wedge \boldsymbol{E}_0 + M_1(n', n)\boldsymbol{\sigma} \wedge \hat{\boldsymbol{k}} - \mathrm{i}\,\mathrm{Im}\, E_1^{\text{pv}}(n', n)\boldsymbol{\sigma}. \tag{27}$$

The two first terms correspond to the Stark-induced dipole; they involve a scalar and a vector transition polarizability. The next term represents the normal magnetic dipole, $\hat{\boldsymbol{k}}$ is a

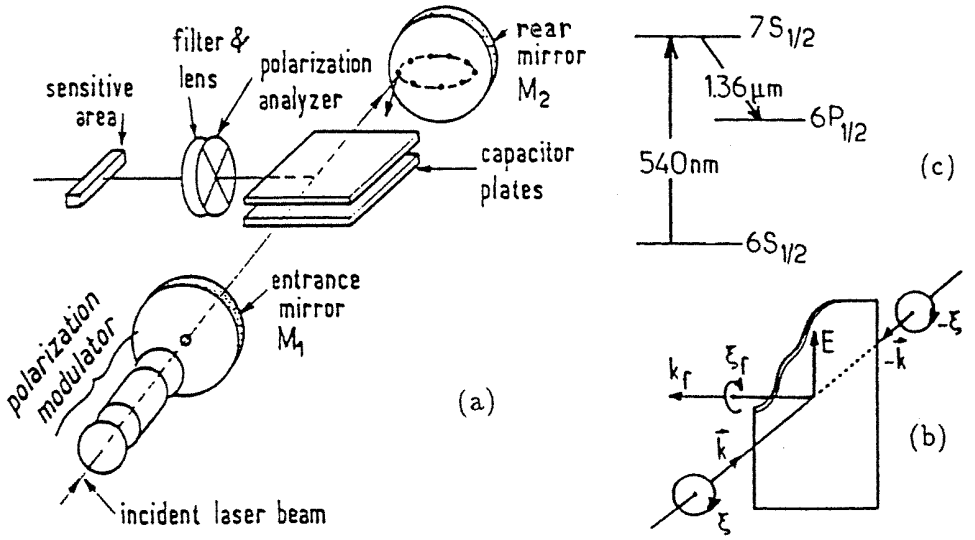

Figure 2. The 1982–83 Paris experiment. (a) The main elements of the apparatus. The polarization modulator is composed of a Pockels cell inserted between two rotating half-wave plates. Mirrors M_1 and M_2 inside the caesium cell allow about 60 double passages of the beam through the vapour with small direction dispersion $< 1^\circ$ (beam impacts shown on mirror M_2. (b) Mirror symmetry of the experiment broken by the circular polarization ξ_f of the fluorescence intensity detected in the direction $\boldsymbol{k}_f$ contained in the symmetry plane. (c) Caesium energy levels involved in the PV experiment.

unit vector collinear to the wavevector of the light beam. The last component, proportional to the electron spin, is a pseudovector while a vector behaviour is expected for an electric dipole. This is a manifestation of the chiral electroweak interaction. When the transition is excited, interferences take place between the various dipole amplitudes $\boldsymbol{d}_{\rm eff} \cdot \hat{\epsilon}$. In general $\hat{\epsilon}$ is a complex unit vector representing a general state of elliptical polarization. Hence a whole wealth of new optical pumping effects can take place. For instance we can consider the atomic orientation, $\boldsymbol{P} = \langle \boldsymbol{\sigma} \rangle$, created in the final state when the transition is excited in a transverse static electric field with circularly polarized light $\hat{\epsilon} = (\hat{x} + \mathrm{i}\xi\hat{y})/\sqrt{2}$. The circular polarization $\xi = \pm 1$ also represents the helicity of the incident photon, i.e. the projection of its angular momentum on its velocity divided by $\hbar c$). From the usual optical pumping rules, we expect a longitudinal orientation proportional to the photon angular momentum, $\boldsymbol{P}_\parallel = -\xi \boldsymbol{k}\beta/\alpha$. However, an unusual transverse orientation is also predicted

$$\boldsymbol{P}_\perp = -2\frac{M_1 + \xi \,\mathrm{Im}\, E_1^{\rm pv}}{\alpha E^2}\boldsymbol{k} \wedge \boldsymbol{E}. \tag{28}$$

Because of the presence in the above expression of the photon helicity ξ, $\boldsymbol{P}_\perp$ does not transform like an angular momentum, under space reflection. This is clearly a manifestation of the breaking of space-reflection invariance in the radiative transition. From these considerations results the basic principle of the 1982 experiment performed at ENS (Bouchiat *et al* 1982, 1984). Counter-propagating beams were used in order to cancel in $\boldsymbol{P}_\perp$ the two M_1 contributions to $\boldsymbol{P}_\perp$. Hence the ratio $P_\perp/P_\parallel$ yields directly the parameter of interest, $\mathrm{Im}\, E_1^{\rm pv}/\beta E \sim 1.5 \times 10^{-5}$ at a typical field strength of 100 V cm^{-1}. The electronic polarization in the 7S state was detected by measuring the circular polarization ratio of the fluorescence light emitted in the direct radiative decay of the $7S_{1/2}$ state via the allowed $7S_{1/2}$–$6P_{1/2}$ transition (1.36μ).

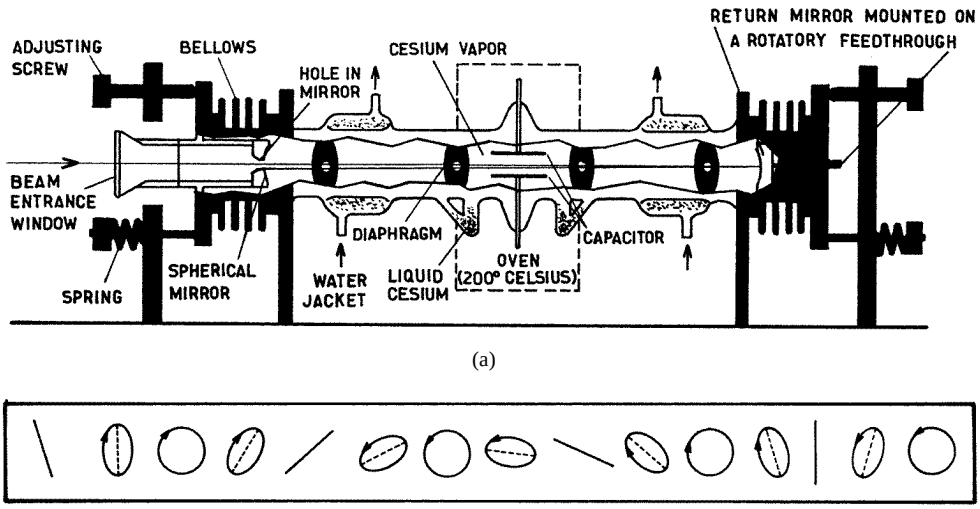

Figure 3. (a) The caesium cell with multipassages of the beam between internal mirrors. (b) The beam polarization at the output of the polarization modulator represented at equal time intervals (Bouchiat *et al* 1985a).

A schematic view of this experiment is shown in figure 2. The forward and backward beams were propagating parallel to the capacitor plates and one observed the fluorescence light emitted in the direction orthogonal to the beams and to the field through a circular polarization analyser. In this way $\boldsymbol{P}_\perp$ was monitored continuously. The detection of $\boldsymbol{P}_\parallel$ was performed during calibration sequences during which a 10 G magnetic field was applied along $\boldsymbol{E}$; the component of $\boldsymbol{P}_\parallel$ which then appeared in the observation direction was thus detected with the same optics and electronics as $\boldsymbol{P}_\perp$.

Two key components of the experimental set-up were a caesium cell with multiple passages of the laser beam between internal mirrors (figure 3(a)) and a triple modulator providing complete characterization of the beam polarization (figure 3(b)). The cancellation of the two M_1 contributions by the multiple passages of the beam played an important role in reducing the systematic effect which might have arised from a linear polarization modulation correlated with the helicity modulation. With the multipass cell one may still worry about the fact that due to the birefringence of the rear mirror the forward and the backward beams have slightly different polarizations. The associated error was made negligible, first by selecting a mirror having a very small birefringence and second by exchanging the slow and fast axes of the birefringence periodically during data acquisition (Bouchiat *et al* 1984). In this experiment the control of geometrical alignment, stray E-fields and light polarization defects was performed using parity-conserving atomic signals. About 30 such signals were recorded simultaneously with the PV signal and exploited in order to reconstruct in real time any systematic asymmetry resulting from the combination of two defects (Bouchiat *et al* 1986). Actually such effects were found to be well below the statistical uncertainty. The effective averaging time was 300 h. The experiment was performed twice, on two different hyperfine structure (hfs) components, a $\Delta F = 0$ and a $\Delta F = 1$ transition, where the observation conditions are very different. The two results were in agreement with each other, within the precision achieved.

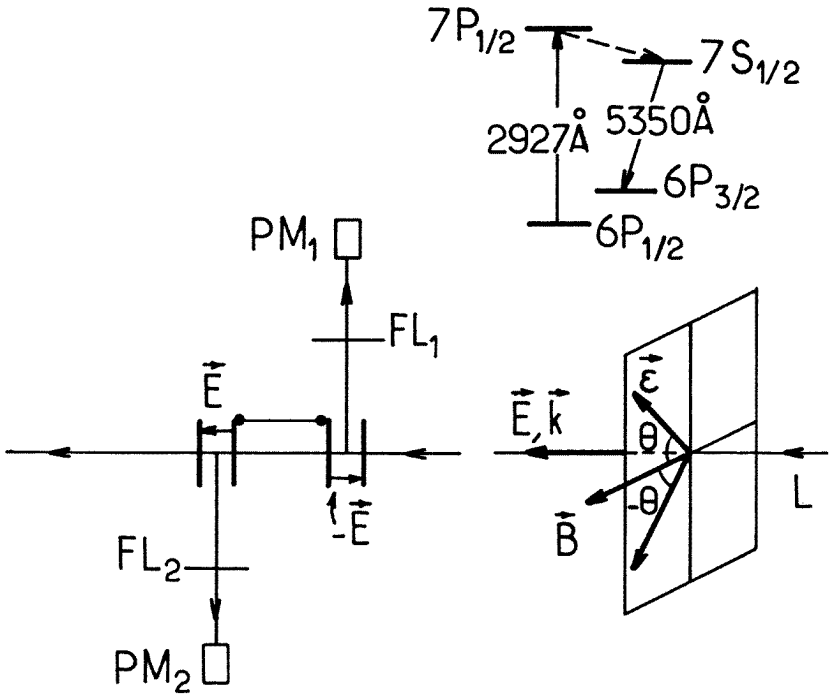

Figure 4. The Berkeley experiment in Tl vapour (Drell and Commins 1985); chiral absorption of plane polarized light. There are two interaction regions with opposite electric fields. L, pulsed narrow-band laser beam; FL, filter and lenses; PM, photomultiplier detecting the $7S \rightarrow 6P_{3/2}$ cascade fluorescence of the $7P_{1/2}$ decay. The atomic levels relevant for this experiment are also represented.

The Paris 1982–83 experiment reached 12% accuracy, all sources of uncertainties being included. It provided the first significant low-energy test of electroweak theory involving electrons and nuclei. There was room for improvement, however, mainly because of the limited angular acceptance of the fluorescence detection system. So we kept thinking about various possibilities of improvements. In fact, in 1979 we had proposed new experiments using static transverse electric and magnetic fields where a pseudoscalar appears this time in the transition probability (Bouchiat *et al* 1979). In the first one the PV effect is a chiral absorption of plane polarized light involving the pseudoscalar quantity $(\boldsymbol{\epsilon}\cdot\boldsymbol{B})(\boldsymbol{\epsilon}\cdot\boldsymbol{E}\wedge\boldsymbol{B})$. This effect was observed later on in the $6P_{1/2}$–$7P_{1/2}$ transition in Tl in a beautiful experiment conducted in 1984–86 by Commins at Berkeley (Drell and Commins 1984, 1985, Tanner and Commins 1986, see figure 4).

In our second suggestion the PV effect is a circular dichroism involving the pseudoscalar quantity $\xi\boldsymbol{k}\cdot\boldsymbol{E}\wedge\boldsymbol{B}$. This is the basic principle of the experiment performed in Cs by Wieman at Boulder which yielded its first results in 1985 (Gilbert *et al* 1985) and improved results in 1988 (Noecker *et al* 1988). Most recently, an upgraded version of this experiment has provided the most precise PV measurements in atoms (see section 3.4).

In order to observe the circular dichroism in transverse $\boldsymbol{E}$ and $\boldsymbol{B}$ fields the Zeeman structure of the $6S_{1/2}$–$7S_{1/2}$ transition must be resolved, otherwise the effect cancels out. For this reason the Boulder group has chosen to work with an atomic beam that they irradiate at right angles (see figure 5). In this way Doppler broadening is greatly reduced and the

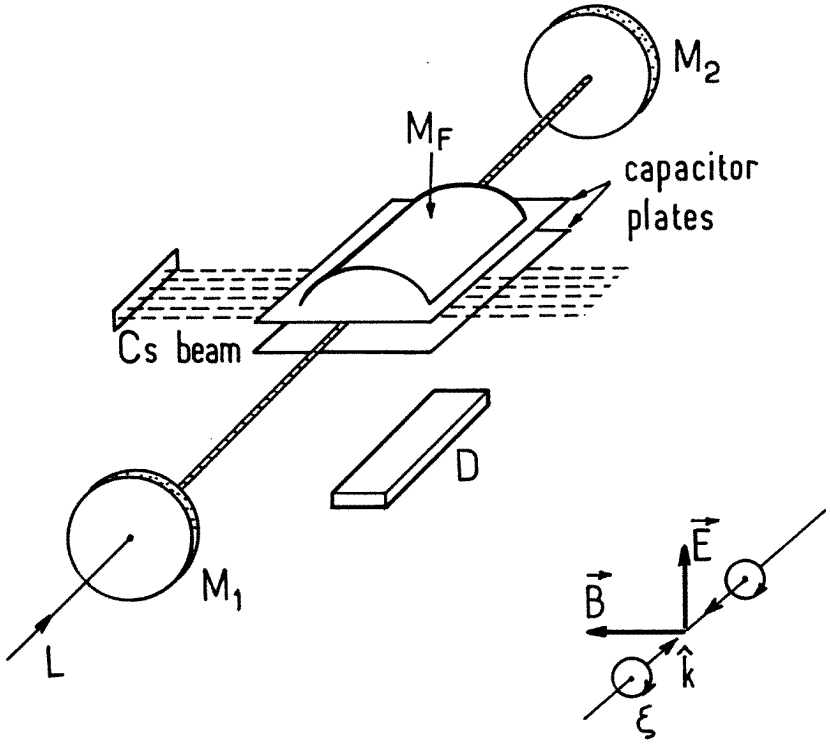

Figure 5. The first version of the Boulder experiment in an atomic caesium beam: circular dichroism in crossed $\boldsymbol{E}$ and $\boldsymbol{B}$ fields (see the sketch of the interaction region). M_1 and M_2, spherical mirrors forming a Fabry–Perot cavity; M_F, light collection mirror; D, detector for the $6P_{1/2,3/2} \rightarrow 6S_{1/2}$ emission following $7S_{1/2}$ decay.

field strength required depends on the collimation of the atomic beam (70 G in the first version of the experiment and 6.4 G in the latest one). Since it is no longer necessary to analyse the polarization of the fluorescence light, in the first version of their experiment they detected all the light emitted in the near infrared in the second step of the $7S_{1/2}$ state radiative decay, at the price of a certain loss in selectivity. The accuracy achieved in 1988 reached 2.5%. We present the upgraded version of this experiment in more detail.

3.4. The presently most accurate PNC experiment

The upgraded version of the Boulder experiment that we now describe has recently provided results of impressive statistical accuracy (Wood *et al* 1997).

The underlying principle of the experiment in its latest version has not changed since 1985; it still relies on the search for the pseudoscalar quantity $\xi \boldsymbol{k} \cdot \boldsymbol{E} \wedge \boldsymbol{B}$ in the absorption cross section of the excitation beam with angular momentum $\xi \boldsymbol{k}$. There are, however, two important differences which improve the experimental sensitivity: the atomic beam is now polarized and the detection scheme has been modified.

The beam passes through three regions: in the first, all the atoms are accumulated in a single Zeeman substate which will interact with the excitation laser. This is achieved by hyperfine and Zeeman pumping in a low magnetic field with two diode laser beams, one being circularly polarized. Next, the atoms pass through the interaction region itself and

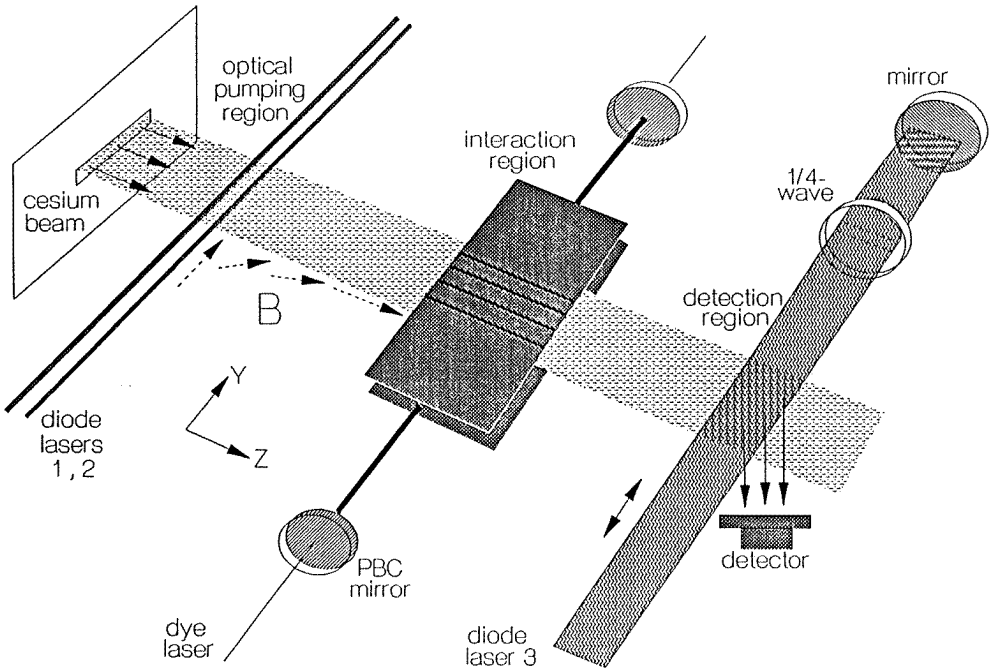

Figure 6. Latest version of the Boulder experiment in caesium, using a polarized atomic beam (Wood *et al* 1997).

finally they enter the detection region. There, atoms belonging to the initially depopulated hyperfine state are detected with high efficiency via resonant scattering of a large number of IR photons. The signal represents therefore the modification of the hyperfine populations in the ground state produced by passing across the interaction region. Its origin is, among other things, the 6S $\rightarrow$ 7S transition. There is no guarantee, however, that it only comes from 7S atoms having made the 6S–7S transition; further discrimination is required. Moreover, the instantaneous signal involves the whole transition probability and not only its pseudoscalar part. The pseudoscalar part, a tiny fraction of this signal ($\sim 6 \times 10^{-6}$), is identified and measured by making periodic reversals of all the parameters which change its sign, namely the electric field, the magnetic field in the pumping region, the laser polarization, the magnetic field in the interaction region, and the circular polarization of the optical pumping light.

Besides the atomic beam, the other key component of the apparatus is a high-finesse (100 000) Fabry–Perot power buildup cavity (PBC) through the centre of which passes the beam of polarized atoms (figure 6). A high speed servosystem locks the green laser frequency to the resonance frequency of the cavity. The cavity itself is kept in resonance with the 6S $\rightarrow$ 7S transition by another servosystem. The PBC not only enhances the transition rate but, in addition, like the multipassage cavity of the Paris experiment, it greatly suppresses the Stark–M_1 interference effect which might give rise to a systematic effect in presence of imperfections in the polarization of the excitation beam. As in the Paris experiment, the rear mirror birefringence is reversed by rotating it periodically so as to exchange the fast and slow axes. There is, however, an important difference. In the Paris multipass cell the transition was excited in a travelling wave which performed a series of forward and backward passages. In the PBC on the other hand, the atoms interact

with a standing wave whose intensity varies spatially across the atomic beam profile. This gives rise to inhomogeneous AC Stark shifts. A typical laser intensity inside the cavity is 1 MW cm^{-2} at the antinodes, which means that the 6S–7S resonance frequency can be shifted by as much as 20 MHz at the peak intensity due to the AC Stark effect. Furthermore, this shift is spatially modulated, and although the atomic beam is highly collimated the atoms have a non-zero velocity along the wavevector $\boldsymbol{k}$. Hence different atoms crossing the light beam with different trajectories experience different AC Stark shifts; to those which undergo the largest shift corresponds the largest transition probability. As a result the line shape for the 6S–7S transition, almost completely determined by AC Stark broadening, is complicated and asymmetric (Wieman *et al* 1987, Cho *et al* 1997). Moreover, any modulation of the AC Stark shift causes a change in this line shape and gives rise to a modulation in the transition rate. In particular, because of the vector spin-dependent part of the static polarizability it so happens that the AC Stark shift $\Delta_{6,7}$ receives a contribution linear in the circular polarization of the beam and in the atomic polarization; $\Delta_{6,7} = \alpha' + \xi\beta'\langle\boldsymbol{\sigma}\rangle \cdot \boldsymbol{k}$. In other words the high intensity inside the PBC allows the Boulder group to obtain an excellent signal-to-noise ratio but with serious side effects. In such circumstances one can easily understand why 20 times more data were taken in the investigation and elimination of the systematic errors than in the actual PNC measurement. Major contributions of signals that mimic PNC involve line-shape distortion factors. The most troublesome systematic error arises from imperfections in the polarization of the green light combined with the distortion in the 6S–7S line shape. The Boulder group has not yet indicated its exact origin, but they do mention that in a block of data it can be as large as $\pm 2\%$ of the PV effect, typically one-half of the statistical uncertainty for this block. 'To keep this error small, we measured and minimized,' they say, 'the polarization imperfection before each block... and we intentionally acquired nearly equal numbers of blocks with positive and negative values of the imperfection in each run.' At first sight, it looks somewhat questionable to use this kind of procedure, to get rid of a systematic effect which might have serious consequences. Indeed, this effect is present on one hfs line only and, hence, it affects directly the difference between the two lines which has important implications (see (31) below). We hope that a more detailed report from the Boulder group will clarify this point.

The quoted accuracy is 3.5×10^{-3} and the result agrees with all previous results to within their respective uncertainties (see table 2). Even more interesting is the comparison of the measurements performed on the two different hfs transitions $6S_{1/2,F=3} \rightarrow 7S_{1/2,F=4}$ and $6S_{1/2,F=4} \rightarrow 7S_{1/2,F=3}$. The difference in E_1^{pv}/β reported for those two transitions, namely $(4.8 \pm 0.7) \times 10^{-2}$ constitute the first evidence for a nuclear spin-dependent electron–nucleus interaction that violates parity. This subject is discussed in section 4.3.

4. The results in caesium and their implications

In this section we are going to examine the present results of experiments and atomic theory in Cs and their implications for electroweak theory. This will make more explicit our motivations for pushing forward other experiments under completion and for devising new projects whose results can contribute further to our knowledge.

4.1. Atomic physics calculations and the present status of the results in caesium

Atomic physics calculations are necessary to extract the weak charge from the experimental data. We can write E_1^{pv} as the product of $(Q_W/-N)$ by a purely atomic quantity,

Table 2. Summary of the results in caesium.

A—experiments*	B—atomic theory computations
$\mathrm{Im}\,E_1^{\mathrm{pv}}(10^{-11}\lvert e\rvert a_0)$	$(-N/Q_{\mathrm{W}})\mathrm{Im}\,E_1^{\mathrm{pv}}(10^{-11}\lvert e\rvert a_0)$
	First principles
$-0.803 \pm 0.095^{(a,b)}$ Paris 82–83	$-0.908 \pm 0.010^{(f)}$ Novosibirsk 89
$-0.867 \pm 0.069^{(c)}$ Boulder 85	$-0.905 \pm 0.009^{(g)}$ Notre Dame 90
$-0.828 \pm 0.020^{(d)}$ Boulder 88	
$-0.837 \pm 0.003_{\mathrm{exp}} \pm 0.006^{(e)}_{\mathrm{theory}}$ Boulder 97	
	Semi-empirical
$^*\beta a_0^3$ from S.E. evaluations	$-0.935 \pm 0.02 \pm 0.03^{(j)}$ Paris 86
$27.19 \pm 0.4^{(h)}$	$-0.904 \pm 0.02^{(k)}$ Oxford 90
$27.17 \pm 0.35^{(i)}$	$-0.895 \pm 0.02^{(l)}$ Paris 91
βa_0^3 from first principles	
$27.00 \pm 0.20^{(m)}$	
$A/B \Longrightarrow Q_{\mathrm{W}}^{\mathrm{exp}} = -72.1 \pm 0.3_{\mathrm{exp}} \pm 0.9_{\mathrm{theory}}$	

(a) Bouchiat *et al* (1982); (b) Bouchiat *et al* (1984); (c) Gilbert *et al* (1985); (d) Noecker *et al* (1988); (e) Wood *et al* (1997); (f) Dzuba *et al* (1989b); (g) Blundell *et al* (1990); (h) Bouchiat and Piketty (1983); (i) Bouchiat and Guéna (1988); (j) Bouchiat and Piketty (1986); (k) Hartley and Sandars (1990); (l) Bouchiat (1991); (m) Blundell *et al* (1992).

$\mathcal{E}_1^{\mathrm{pv}} = E_1^{\mathrm{pv}}/(Q_{\mathrm{W}}/-N)$ (the neutron number N is introduced here just for convenience, the ratio $Q_{\mathrm{W}}/-N$ being close to unity). The quantity $\mathcal{E}_1^{\mathrm{pv}}$ can be considered as an infinite sum over the intermediate P states admixed with the S states by the parity-violating interaction

$$\mathcal{E}_1^{\mathrm{pv}} = \left(-\frac{N}{Q_{\mathrm{W}}}\right)\sum_n \frac{\langle 7\mathrm{S}_{1/2}|d_z|n\mathrm{P}_{1/2}\rangle\langle n\mathrm{P}_{1/2}|V_{\mathrm{pv}}|6\mathrm{S}_{1/2}\rangle}{E(6\mathrm{S}_{1/2}) - E(n\mathrm{P}_{1/2})} + \text{ crossed terms.}$$

The atomic orbitals and the valence-state energies are perturbed by many-body effects. To date, two different approaches have been employed, one starting from first principles and the second semi-empirical. In the first case the Dirac equation is solved for a single electron in a Hartree–Fock potential and the many-body corrections are computed perturbatively (with resummation of specially chosen sets of diagrams). The second approach incorporates in a consistent way a wealth of empirical data available from the numerous spectroscopic measurements performed in Cs, namely information regarding energies of the valence states, allowed-dipole matrix elements and hfs splittings of the $\mathrm{S}_{1/2}$ and $\mathrm{P}_{1/2}$ states. In this way atomic many-body perturbation theory is needed only to compute small correction terms.

The results in caesium are presented in table 2. Experimental values of $\mathrm{Im}\,E_1^{\mathrm{pv}}$ are deduced from the measured PV parameter $\mathrm{Im}\,E_1^{\mathrm{pv}}/\beta$, combined with the value of β obtained from two independent semi-empirical determinations compatible with the theoretical prediction. The experimental accuracy has improved by successive steps from 12% in our first 1982–1983 experiment to 0.35% most recently in the latest version of the Boulder experiment, but all results are in agreement with each other to within the quoted uncertainty. However, for β we remain with an uncertainty of 0.7%.

Concerning atomic physics theoretical results there are two computations using the first-principles approach by the Novosibirsk group (Dzuba *et al* 1989b) and by the Notre Dame group (Blundell *et al* 1990). They agree with each other, each one reaching an accuracy of 1%. This is a real *tour de force* and in this respect we should stress the pioneering work of the Novosibirsk group (Dzuba *et al* 1989a), the first to show that relativistic many-body computation in Cs could be pushed to the 1% precision level using techniques inspired from field theory. The work of the Notre Dame group was much more

than a mere confirmation. By using very advanced numerical methods they arrived at an exact treatment of two electron–hole pair excitation. (For a review presentation of these calculations see also Blundell *et al* (1991).) The calculations by the semi-empirical approach (Bouchiat and Piketty 1986, Hartley and Sanders 1990) have now reached an accuracy of 2% which is limited by the uncertainty associated with some of the empirical inputs (the allowed E_1 amplitudes). This should improve once more precise measurements have been performed. The agreement obtained by the two approaches further reinforces our confidence in the final result. However, the recent Boulder result issues a new challenge to atomic physics theorists; reduce the theoretical uncertainty from 1% to $\frac{1}{3}$% in order to match the experimental precision.

The contribution induced by Z^0 exchange between electrons must also be included. Although expected to be small compared to the basic PNC effect associated with the nucleus–electron Z^0 exchange because of Coulomb repulsion, it has been computed precisely (Blundell *et al* 1992). It amounts to 3×10^{-4} of the main contribution. Therefore Z^0 exchange between electrons can be safely neglected.

In conclusion, by combining the experimental result of Wood *et al* (1997), $E_1^{\rm pv}/\beta = 1.5935 \pm 0.0056$ mV cm^{-1} with the atomic theoretical results of Blundell *et al* (1992), $-N/Q_{\rm W}\,{\rm Im}\,E_1^{\rm pv} = -0.905 \pm 0.009(10^{-11}|e|a_0)$ and $\beta/a_0^3 = 27.00 \pm 0.20$, we presently obtain an empirical value of $Q_{\rm W}({\rm Cs})$ whose current accuracy is limited essentially by atomic theory

$$Q_{\rm W}^{\rm ex} = -72.1 \pm 0.3_{\rm exp} \pm 0.9_{\rm theory}. \tag{29}$$

4.2. Implications for electroweak theory

4.2.1. Model-independent interpretation. The most direct implication of a precise determination of the weak nuclear charge concerns the determination of the fundamental constants $C_{\rm u}^{(1)}$, and $C_{\rm d}^{(1)}$ appearing in the phenomenological Lagrangian describing the PV electron–hadron interaction involving energy momentum transfer squared q^2 such that $|q^2| \ll M_{Z_0}c^2$. These constants used by particle physicists are simply related to the weak charges of the quarks: $C_{\rm u}^{(1)} = -\frac{1}{2}Q_{\rm W}({\rm u})$ and $C_{\rm d}^{(1)} = -\frac{1}{2}Q_{\rm W}({\rm d})$. In a model independent analysis, the empirical determination of $Q_{\rm W}({\rm Cs}) = 188Q_{\rm W}({\rm u}) + 211Q_{\rm W}({\rm d})$ (from (12)) defines an allowed band in the $(C_{\rm u}^{(1)}, C_{\rm d}^{(1)})$ plane. The high-energy SLAC experiment measures a left–right asymmetry $A_{\rm LR}$ in highly inelastic polarized-electron scattering on deuterons (Prescott *et al* 1978, 1979). It turns out that at such energies the target is broken into its fundamental constituents so that the quarks act incoherently. $A_{\rm LR}$ then involves the following electroweak interference term

$$Q_{\rm e}({\rm u})Q_{\rm W}({\rm u}) + Q_{\rm e}({\rm d})Q_{\rm W}({\rm d}) = \tfrac{2}{3}Q_{\rm W}({\rm u}) - \tfrac{1}{3}Q_{\rm W}({\rm d}).$$

One sees immediately (figure 7) that the band defined by the SLAC experiment is nearly orthogonal to that obtained from atomic physics. This illustrates the complementarity of the two types of experiments. The high-energy band is also larger, this is partly so because the result is obtained from a two-parameter fit; indeed there is another contribution to $A_{\rm LR}$ involving the pseudovector coupling quark–Z^0. We expect new polarized electron scattering experiments will soon improve upon the precision of the SLAC results.

The predictions of the standard model for the various values of $\sin^2\theta_{\rm W}$ are represented in figure 7 by a segment. It is worth noting that it intercepts the intersection region for a value of $\sin^2\theta_{\rm W}$ which is close to the world average.

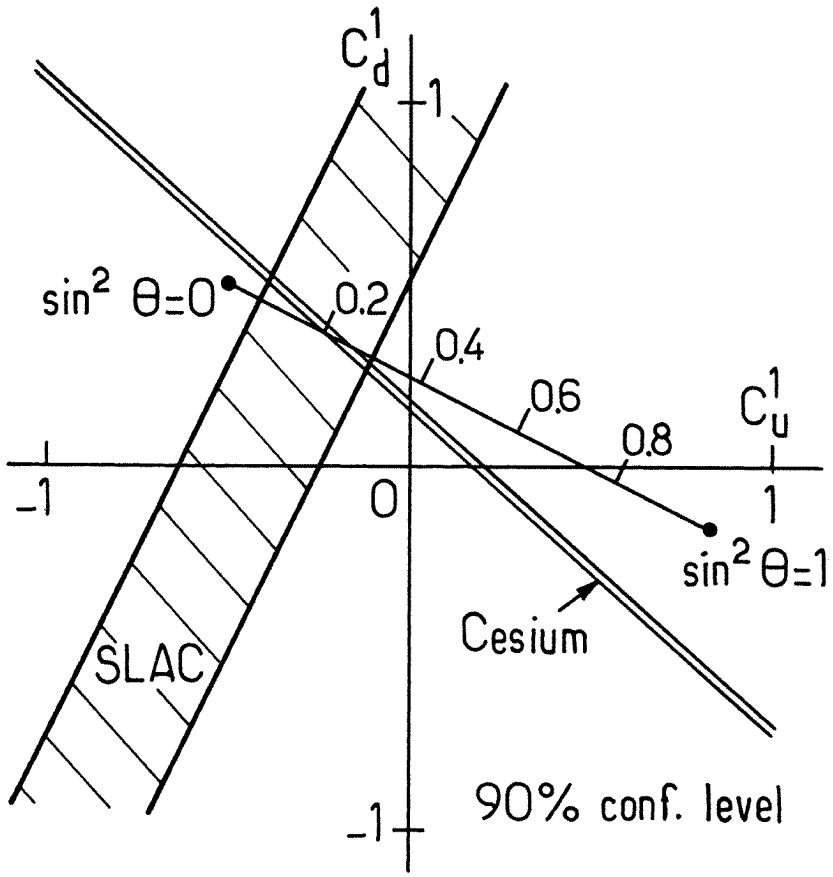

Figure 7. Experimental, model-independent determination of the weak charges of the u and d quarks. The two bands represent the domains allowed by the high-energy SLAC and by the caesium experiments. The graduated segment represents the prediction of the standard model for values of the parameter $\sin^2\theta$ from 0 to 1.

4.2.2. Comparison with the standard model prediction. Since Q_W is a fundamental quantity it must be compared with the value predicted by the standard model. In order to incorporate electroweak radiative corrections, the theory being renormalizable, for a complete definition of the theory it is necessary to fix a certain number of constants, three in fact. We choose α, G_F and as the third constant the most natural choice is the mass of the Z^0 boson, M_{Z_0}. With such a choice, the sensitivity of the radiative corrections to the top mass, via vacuum polarization loop diagrams which involve $(m_t/M_W)^2$ terms (Veltman effect), practically disappears†. This dependence even cancels out for the particular ratio of protons to neutrons involved in natural caesium, $^{133}_{55}$Cs. The theoretical value of Q_W (Marciano and Sirlin 1984) is given by

$$Q_W^{th} = -73.20 \pm 0.13 \tag{30}$$

† *An historical note*: before the LEP era, instead of M_{Z_0}, people chose the ratio M_W/M_{Z_0} as the third electroweak constant, since it could be derived from neutrino physics. With such a choice, Q_W^{th} involves the top quark mass and atomic PV results were used to obtain the bound $m_t < 190$ GeV/c^2. This is to be compared with the current value of 175 GeV/c^2, deduced from the recent direct observation of the top quark at Fermilab.

where the uncertainty comes from hadronic physics. We note that the difference from the experimental value $\delta Q_W = Q_W^{ex} - Q_W^{th} = 1.1 \pm 0.9$ is close to one standard deviation. This is a remarkable result if one considers the difference of some ten orders of magnitude between the values of q^2 at which the determinations of M_Z and Q_W were carried out. Such a result demonstrates the success of the standard model over this extremely wide range.

4.2.3. Constraints regarding an extra Z^0 boson. At present it would appear beyond the reach of atomic physics results to compete with LEP data in a test of q^2 radiative corrections of pure electroweak origin (Altarelli 1991, Peskin and Takeuchi 1992). In fact the major merit of atomic physics results is their ability to test q^2-dependent effects. In particular, most alternatives to the standard model make the assumption of a second neutral vector boson Z'^0. While the LEP data are sensitive to the Z'^0 only through its mixing with the Z^0 boson, the atomic physics data receive a contribution whatever the degree of Z^0–Z'^0 mixing and even when there is no mixing whatsoever (Altarelli 1991, Lagacker and Luo 1992). The corresponding modification of Q_W is proportional to $(M_{Z_0}/M_{Z_0'})^2$. Several theorists have analysed the present results. In a specific model Altarelli (1991) finds that the lower limit on $M_{Z_0'}$ coming from Q_W^{ex} with the present uncertainty is 360 GeV/c^2 while a direct Fermilab measurement leads to a somewhat lower limit 288 GeV/c^2.

In the above discussion the mass of the new vector boson was assumed to be infinite on an atomic scale. The possible existence of a new light vector boson U cannot be discarded. The search for a very very light U boson, $\hbar/(M_U c) > 1$ m, has been pursued actively in experiments looking for a breaking of the principle of equivalence due to a possible 'fifth force'. Atomic physics offers the possibility of exploring the range $M_U \geqslant 0.1$ MeV/c^2. As an illustration, we shall briefly discuss a simple model proposed by Fayet (1977, 1979, 1980, 1986a,b,c, 1990) in connection with the problem of supersymmetry breaking. The modification of the weak charge is given by

$$\Delta Q_W(U) = 3(Z+N) r^2 \cos\varphi R(M_U).$$

The parameter r $(0 \leqslant r^2 \leqslant 1)$ is the ratio of the electroweak gauge-breaking energy scale to the corresponding scale for the U boson gauge group and $\cos\varphi$ gives the ratio of the vector to pseudovector coupling with matter particles. The atomic factor $R(M_U)$ has been computed by Bouchiat and Piketty (1983) and is listed in table 3 for typical values of M_U.

Table 3. Atomic factor $R(M_U)$ for the weak charge correction $\Delta Q_W(U)$ in caesium.

M_U (MeV/c^2)	0.2	1.0	2.4	10	$\geqslant$100
$R(M_U)$	0.08	0.33	0.5	0.72	1.0

Using the deviation δQ_W from the standard model prediction one obtains the following constraints

$$2.5 \times 10^{-4} \leqslant r^2 \cos\varphi R(M_U) \leqslant 4.9 \times 10^{-3}.$$

When r^2 lies close to 1, one can conclude that for $M_U \geqslant 1$ MeV/c^2 the U boson couples mostly as a pseudovector. It is interesting to consider the production rates of the U boson by high-energy particles when M_U is say $\leqslant$100 MeV/c^2. For vector coupling, the rate is proportional to $\alpha r^2 \cos\varphi (M_U/M_W)^2$, while in the pseudovector case the rate is governed by the quantity $\alpha r^2 (m_f/M_W)^2$ where m_f is the mass of the matter constituents. With the values taken for M_U, the production rate via vector coupling is negligible. The pseudovector

rate behaves very differently; it is independent of M_U and becomes measurable in the decay of heavy quark–antiquark bound states (quarkonium)†. The complementarity of the two approaches is quite evident in this simple example since high-energy experiments are sensitive only to the pseudovector coupling, while atomic parity-violation experiments measure the interference between the vector and the pseudovector couplings.

4.2.4. Constraints on exotic particles such as the recently suggested leptoquarks. There has been considerable excitement among the high-energy community, in the last few months, about what is known as the HERA anomaly. Two experiments (Adloff *et al* 1997, Breitweg *et al* 1997) at the HERA collider in Germany have found an excess of events (24 observed as opposed to 14 predicted by the standard model) in deep inelastic positron–proton scattering. The anomaly occurs in a region of high-momentum transfer that has not been explored previously, but in which the predictions of perturbative quantum chromodynamics are expected to be reliable. Besides the obvious explanation by a statistical fluctuation, the most popular interpretation involves the existence of a leptoquark, a spin-0 particle with a mass around 200 GeV/c^2 that carries both a baryonic and a leptonic charge. The favoured realization of the leptoquarks are the squarks, $\tilde{q}$, spin-0 supersymmetric partners of the quarks q in the case where the so-called 'R-parity' is not conserved. Very recent experiments, performed at the Fermilab Tevatron (Kambara *et al* 1997, Norman *et al* 1997) have found no evidence for leptoquark pair production and have placed rather stringent lower limits on leptoquark masses. Among the various squarks, the remaining candidate for an explanation of the HERA anomaly, at the time of the writing, seems to be the 'stop' $\tilde{t}_L$ produced in the channel $e^+ + d \rightarrow \tilde{t}_L$. The subscript L (for left) means that the stop is a linear combination of a scalar and a pseudoscalar particle. At low energies the exchange of leptoquarks generates new electron–quark contact interactions which contribute to the PNC electron–nucleus potential. The deviation of the measured weak charge, Q_W^{exp}, from the standard model prediction, i.e. the quantity $\delta Q_W = Q_W^{exp} - Q_W^{th}$, provides an upper bound on the ratio of the fermion–leptoquark coupling constant to the leptoquark mass. With the new Q_W^{exp} value from the latest Boulder experiment, the constraint is already rather tight, but it will become even more severe if the theoretical uncertainty affecting Q_W^{exp} is reduced by improved atomic physics computations. The above considerations provide further evidence of the links between high-precision measurements of atomic parity violation and high-energy particle physics.

4.3. The nuclear spin-dependent electron–nucleus PV interaction

The study of the nuclear spin-dependent electron–nucleus PV interaction constitutes another motivation for precise PV atomic measurements. Indeed, from measurements performed on different hfs lines, the spin-dependent and spin-independent contributions can be separated unambiguously. The separation of the effects does not require any improvement in atomic theory. In the case of caesium it is convenient to introduce the measurable physical quantity:

$$r_{hf} = \frac{E_1^{PV}(6S\text{–}7S, \Delta F = -1)}{E_1^{PV}(6S\text{–}7S, \Delta F = +1)} - 1. \tag{31}$$

A non-zero experimental value of r_{hf} provides a diagnosis of a nuclear spin-dependent contribution. The most significant result of the recent Boulder experiment is certainly the

† Fayet has used experimental limits on U boson production in ψ and Υ decays to place the following bound: $r^2 < \frac{1}{2}$.

first evidence, to within 14% accuracy, for a nuclear spin-dependent PNC electron–nucleus interaction. Specifically

$$r_{\rm hf} = (4.8 \pm 0.7) \times 10^{-2}.$$

The most obvious origin for such an electron–nucleus interaction would be a Z_0 exchange process involving a pseudovector Z^0–nucleus coupling with a vector Z^0–electron coupling. However, due to what is apparently a numerical accident, this mechanism is strongly suppressed in the standard electroweak model.

A nuclear spin-dependent PV electron–nucleus interaction (Flambaum and Khriplovich 1985, Kozlov 1988, Bouchiat and Piketty 1991a) is generated by the hyperfine coupling perturbation upon the nuclear spin-independent PV interaction involving the weak charge of the nucleus. This effect is of the order of $\alpha G_{\rm F} A^{2/3}$ where A is the atomic number and for the case of caesium it is about the same size as the above Z^0 exchange contribution.

In fact the dominant physical process comes from another mechanism the contamination of the atom—via photon exchange—by the parity-violating processes taking place inside the nucleus. Under the influence of PV nuclear forces, a parity-violating component of the electromagnetic current is generated. It is convenient to define the PV classical electromagnetic current of the nucleons $\boldsymbol{J}_{\rm PV}(\boldsymbol{r}) = \langle \tilde{N}|\boldsymbol{j}_{\rm em}(\boldsymbol{r})|\tilde{N}\rangle$ where $|\tilde{N}\rangle$ is the nuclear ground state perturbed by the PV nuclear forces and $\boldsymbol{j}_{\rm em}(\boldsymbol{r})$ the electric current operator. Zel'dovich (1957) showed that the long-range behaviour, on a nuclear scale, of the electromagnetic field generated by $\boldsymbol{J}_{\rm PV}(\boldsymbol{r})$ is governed by the anapole moment $\boldsymbol{a}$

$$\boldsymbol{a} = -\pi \int {\rm d}^3 r\, r^2 \boldsymbol{J}_{\rm PV}(\boldsymbol{r}) \tag{32}$$

and he proved the following theorem. In the limit of a point-like nucleus the interaction of an atomic electron with the current $\boldsymbol{J}_{\rm PV}(\boldsymbol{r})$ is given by the contact interaction

$$H_{\rm an} = |e|\boldsymbol{a} \cdot \boldsymbol{\alpha}_{\rm e} \delta^3(\boldsymbol{r}) \tag{33}$$

where $\boldsymbol{\alpha}_{\rm e}$ is the Dirac velocity operator of the electron. The rather remarkable fact is that the interaction of the electron with $\boldsymbol{J}_{\rm PV}(\boldsymbol{r})$ not only mimics the Z^0 boson exchange process considered above but leads to a contribution five times larger in the case of caesium.

It turns out that the convection currents play a limited role in $\boldsymbol{J}_{\rm PV}(\boldsymbol{r})$ so that a description in terms of a PV nuclear magnetism is both close to the actual physical situation and conceptually more transparent. Under the influence of PV nuclear forces, the nuclear magnetization distribution inside the nucleus acquires a chiral component $\boldsymbol{\mathcal{M}}_{\rm PV}(\boldsymbol{r})$. Within the general framework of the single-particle model for finite nuclei, it has been shown (Bouchiat and Piketty 1991b) that $\boldsymbol{\mathcal{M}}_{\rm PV}(\boldsymbol{r})$ can be deduced from the normal spin magnetization $\boldsymbol{\mathcal{M}}_{\rm S}(\boldsymbol{r})$ by a rotation around $\boldsymbol{r}$ of a small angle $\beta(r)$:

$$\boldsymbol{\mathcal{M}}_{\rm PV}(\boldsymbol{r}) = \beta(r)\frac{\boldsymbol{r}}{r} \wedge \boldsymbol{\mathcal{M}}_{\rm S}(\boldsymbol{r}) \tag{34}$$

where $\beta(r) \propto r$ when $r \to 0$.

The parity-violating current $\boldsymbol{J}_{\rm PV}(\boldsymbol{r})$ is then nothing but the Ampère current associated with the chiral magnetization $\boldsymbol{\mathcal{M}}_{\rm PV}(\boldsymbol{r})$. The anapole moment $\boldsymbol{a}$ is hence given by

$$\boldsymbol{a} = -\pi \int {\rm d}^3 r\, r^2 \nabla \wedge \boldsymbol{\mathcal{M}}_{\rm PV}(\boldsymbol{r}).$$

By performing an integration by parts one easily obtains the familiar looking formula

$$\boldsymbol{a} = 2\pi \int {\rm d}^3 r\, \boldsymbol{r} \wedge \boldsymbol{\mathcal{M}}_{\rm PV}(\boldsymbol{r}). \tag{35}$$

To within a constant, the anapole moment is related to the chiral magnetization $\mathcal{M}_{\rm PV}(\boldsymbol{r})$ in the same way that an ordinary magnetic moment is related to an electric current density distribution. Figure 8 will help to visualize the chiral magnetic lines within a classical model of the nuclear spin magnetization.

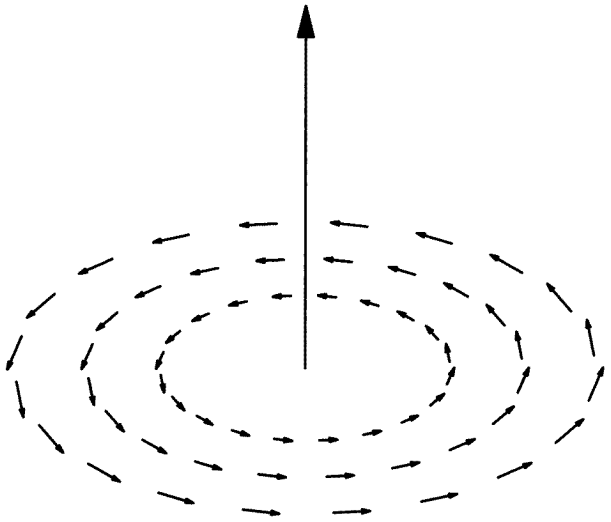

Figure 8. An artist's view of the chiral nuclear magnetization using a classical model of the nuclear spin magnetization. The normal magnetization $\mathcal{M}_{\rm S}(\boldsymbol{r})$ is assumed to be a constant vector parallel to the nuclear spin direction (vertical arrow), distributed uniformly inside a sphere. The chiral magnetization $\mathcal{M}_{\rm PV}(\boldsymbol{r})$ is obtained by rotating $\mathcal{M}_{\rm S}(\boldsymbol{r})$ through the small angle $\beta(r)$ around $\boldsymbol{r}$. Three chiral magnetization lines in the equatorial plane of the nucleus are shown. The vertical normal magnetization, six orders of magnitude larger, is not represented. The vertical anapole moment is given to within a constant by the magnetic moment obtained by identifying the magnetization lines with lines of electric current.

Let us sketch the basic procedure to arrive at the above physical picture and validate it as a practical method of computation (Bouchiat and Piketty 1991b). The first step is to perform on the one-particle nuclear Hamiltonian the infinitesimal $\boldsymbol{r}$-dependent spin rotation:

$$\psi(\boldsymbol{r}) \to \left(1 - \frac{\mathrm{i}}{2r}\beta(r)\boldsymbol{\sigma}\cdot\boldsymbol{r}\right)\psi(\boldsymbol{r})$$

where $\psi(\boldsymbol{r})$ is the nucleon field operator and $\beta(r)$ is assumed to be of first order in $G_{\rm F}$. The above transformation generates from the kinetic energy term a new PV one-nucleon potential; it is to be added to the one-nucleon PV potential associated with the two-body PV nuclear forces

$$V_{\rm pv}^{N}(r) = \frac{G_{\rm F}}{2\sqrt{2}M} g_N \rho(r)\boldsymbol{\sigma}\cdot\boldsymbol{p} + \mathrm{HC}$$

where $\rho(r)$ is the nuclear density distribution. One then determines $\beta(r)$ by requiring the transformed one-nucleon PV potential to give a null result when acting on the single nucleon valence wavefunction relative the nucleus ground state; this condition is sufficient to eliminate the single nucleon PV potential *from the computation of a PV static property of the nucleus*. The angle $\beta(r)$ is found to obey a second-order linear inhomogeneous differential equation involving $\rho(r)$ and the radial wavefunction of the ground-state valence

nucleon. As expected, the infinitesimal space rotation giving $\boldsymbol{\mathcal{M}}_{\rm PV}(\boldsymbol{r})$ is just the space rotation associated with the above spin rotation. Up to a 5% correction associated with convection currents, the anapole moment is given by (35), within the single-particle model of the nucleus. (The spin–orbit coupling is simply accounted for by multiplying $\beta(r)$ by a surface correction term $K_{\rm so}(r)$.)

As in the case of the weak charge $Q_{\rm W}$, atomic computations are necessary to extract the anapole moment $\boldsymbol{a}$ from the ratio $r_{\rm hf}$. $\boldsymbol{a}$ is conventionally expressed in terms of the dimensionless scalar quantity $\kappa_{\rm a}$ defined by

$$|e|\boldsymbol{a} = \langle \boldsymbol{I} \rangle \frac{I+1/2}{I(I+1)}(-1)^{I+1/2+l}\kappa_{\rm a} \tag{36}$$

where l stands for the orbital momentum of the valence nucleon. It turns out that if one takes the ratio of the weak amplitudes appearing in $r_{\rm hf}$ many atomic uncertainties cancel each other out. All atomic computations (Frantsuzov and Khriplovich 1988, Kraftmakher 1988, Bouchiat and Piketty 1991b, Blundell *et al* 1992) used to extract $\kappa_{\rm a}$ from $r_{\rm hf}$ agree with each other to within a few per cent. After subtraction of the two non-dominant contributions to $r_{\rm hf}$ mentioned above, one obtains the following value

$$\kappa_{\rm a} = 0.36 \pm 0.06. \tag{37}$$

The first evaluation of the nuclear spin-dependent effect was given by Flambaum and Khriplovich (1980), Flambaum *et al* (1984). More detailed computations with increasing sophistication in the nuclear physics treatment, have been performed by many authors (Haxton *et al* 1989, Bouchiat and Piketty 1991a,b, Sushkov and Telitsin 1993, Dmitriev *et al* 1994, Flambaum and Vorov 1994, 1995, Dmitriev and Telitsin 1997). These have included many-body nuclear effects: improved two-body short-range correlation, nuclear configuration mixing corrections, renormalization of the PV one-nucleon potential. It is outside the scope of the present review to discuss in any detail these different contributions. The only thing we might say is that the purely nuclear physics uncertainties are not likely to exceed 50%. The authors of the more recent computations (Dmitriev and Telitsin 1997) estimate their uncertainties to be even less than 20%.

The parity nuclear forces are described in terms of one-meson exchange potentials. They involve the PV meson–nucleon coupling constants which are not directly accessible to experiments. Two sets of PV couplings constants (a) and (b) are available in the literature. The set (a) is the result of a fit by Adelberger and Haxton (1985) of PV data coming from p–p, p–α, p–d scattering and radiative transitions in ^{18}F, ^{19}F and ^{21}F nuclei. The second set (b) is a purely theoretical one, proposed by Desplanques, Donoghue and Holstein (Desplanques *et al* 1980), and known in the literature as 'DDH best values'. A computation of the caesium anapole moment performed with the two sets using the same nuclear physics ingredients (Bouchiat and Piketty 1991b) gives for the set (a) a value 50% smaller than the one obtained with the set (b).

In view of the above uncertainties and the dispersion of the published theoretical results, it is fair to say that the Boulder experiment is in semi-quantitative agreement with the theoretical predictions. It turns out that the anapole moment depends in practice only upon two PV meson–nucleon coupling constants, F_π and F_0, associated respectively with the pion and rho exchange. It is then clear than the anapole moment measurement provides a new handle for the study of parity-violating forces in nuclei (Flambaum and Murray 1997).

5. A new generation of experiments in progress and plans for future projects

Current atomic PV experiments now under completion and those planned for the future are motivated by the considerations presented in the preceding section. In brief there are three goals to be reached.

(i) Other accurate measurements of E_1^{pv} in a reliably calculable atom, with the view of making other precise tests of electroweak theory at low-energy cross-checking the recent Boulder result.

(ii) Accurate measurements on different hfs components as a means of identifying again the nuclear spin-dependent PV interaction in Cs as well as in other atoms.

(iii) Precise measurements of E_1^{pv} on atoms belonging to a chain of isotopes of the same element.

The first two goals are being pursued simultaneously for Cs in an experiment in progress at Paris that we describe below. Another possibility is being explored in the Ba^+ ion trapped in an ion trap at Seattle (Fortson 1993). Other possibilities like an experiment in francium, for which E_1^{PV} is 18 times larger than in caesium (Dzuba *et al* 1995), require long-term investment. Even so, impressive efforts have begun in order to improve our knowledge of relevant spectroscopic data (Simsarian *et al* 1996, Zhao *et al* 1997, Lu *et al* 1997) and to initiate experimentation in francium over long periods.

The third goal is considered as a means of achieving a test of electroweak theory free from any uncertainty coming from atomic physics calculations (Fortson *et al* 1990); in the ratio of the measured PV amplitudes relative to different isotopes, the atomic factor is supposed to be eliminated. However this is true only in a first approximation. Nuclear physics theorists (Pollock *et al* 1992, Chen and Vogel 1993) have shown that important uncertainties may arise from the weak charge distribution, i.e. in practice from the neutron distribution inside the nucleus. The variations from one isotope to another affect the precision of the interpretation, the heavier the atom, the larger the uncertainty. In Cs the uncertainty ($\leqslant 10^{-3}$) is sufficiently small to allow us to use measurements performed on two isotopes for testing whether the weak charge is carried out by the neutrons as predicted by the standard model (Chen and Vogel 1993). Because there is a single stable Cs isotope, there is a strong motivation for performing measurements on radioactive Cs isotopes. Therefore, as a prologue, experiments are starting to cool and trap optically radioactive alkali atoms (Gwinner 1994, Lu 1994, Vieira 1994) and even francium (Lu *et al* 1997). Conversely, if one supposes the standard model to be verified, a measurement on a chain of isotopes would provide a unique way of probing the neutron distribution in heavy nuclei: this appears particularly interesting for species having possibly high nuclear deformations and a tendency to repel the neutrons towards their outer surface (VMB Collaboration 1995, Suzuki *et al* 1995). The best examples are dysprosium where experiments are under way (DeMille *et al* 1994, see section 5.2.1) and ytterbium where a proposed experiment (DeMille 1995, see section 5.2.2) has now begun, both elements Dy and Yb having chains of seven stable isotopes. We wish to stress that most of the experiments discussed in this section correspond to experimental situations radically different from those which have already produced data and which were previously analysed (section 3).

Moreover, we shall also consider in this section a closely related objective which is to observe a new manifestation of parity violation; extremely small energy differences between the two enantiomers of a chiral molecule. As previously mentioned, these are particularly intriguing because of their possible link with the appearance of a chirality in living organisms and perhaps even to the origin of life.

5.1. The new Paris experiment in the $6S_{1/2} \rightarrow 7S_{1/2}$ Cs transition based on detection via stimulated emission

Our new method in Paris is to replace the fluorescence method of detection by one based on the observation of the stimulated emission caused by a second laser beam tuned to resonance with the $7S_{1/2}$–$6P_{3/2}$ transition. The detection efficiency is greatly improved since all atoms are forced to emit in the direction of the probe beam. To take full advantage of the method the only constraint is that the probe amplification reach or exceed unity; otherwise the atomic signal would be overwhelmed by the probe intensity and the asymmetry appearing in the transmitted probe intensity would be seriously diluted. In practice this condition is achieved by employing short, intense pulses of excitation light to create a large $7S_{1/2}$–$6P_{3/2}$ population inversion in a time short compared with the $7S_{1/2}$ lifetime. In addition, if one chooses the excitation and probe beams colinear, the interaction region can be made long. An electric field, colinear with the beams, controls the transition probability and hence the probe amplification.

5.1.1. Origin of the left–right asymmetry. In this experiment the left–right asymmetry manifests itself as a rotation of the principal axes of the refractive index of the excited vapour (Bouchiat *et al* 1985b). (Note that the imaginary part of the refractive index is just the gain.) With a linearly polarized excitation beam the excited vapour is prepared with two planes of symmetry. However, as a result of parity violation, its principal axes do not lie in those symmetry planes. They deviate from them by a small angle θ^{PV} and this angle $\theta^{\mathrm{PV}} = -\mathrm{Im}\, E_1^{\mathrm{PV}}/\beta E$, odd under reversal of the electric field, is the PV parameter to be determined experimentally. As a consequence of this deviation angle, the gain of a linearly polarized probe beam is different according to whether its polarization $\boldsymbol{\epsilon}_{\mathrm{pr}}$ lies at 45° or -45° to the excitation beam polarization $\boldsymbol{\epsilon}_{\mathrm{pr}}$. In other words, the two mirror-image experimental configurations represented at the bottom of figure 9 lead to different gains of the probe beam. This reflects the existence of a pseudoscalar contribution to the gain proportional to $\beta\, \mathrm{Im}\, E_1^{\mathrm{PV}}(\boldsymbol{\epsilon}_{\mathrm{ex}} \cdot \boldsymbol{\epsilon}_{\mathrm{pr}})(\boldsymbol{E} \cdot \boldsymbol{\epsilon}_{\mathrm{ex}} \wedge \boldsymbol{\epsilon}_{\mathrm{pr}})$.

This is the basic principle of the measurement which consists precisely of a comparison of the optical gains for two situations which differ only by the plus or minus sign of the 45° angle between the excitation and probe polarizations. To this end the vapour is irradiated with a coherent linear superposition of these two configurations: i.e. $\boldsymbol{\epsilon}_{\mathrm{pr}}$ and $\boldsymbol{\epsilon}_{\mathrm{ex}}$ at the cell entrance are set either parallel or perpendicular. At the output a two channel polarization analyser splits the probe beam in two orthogonally directed beams, each one being polarized at $\pm 45^\circ$ to the incoming beam. In this way the information relative to each one of the two configurations to be compared is switched towards two distinct photodetectors (figure 9). For each reference probe pulse, with no 7S excitation, the exact balance between the two signals S_1 and S_2 is verified. For every probe pulse immediately following an excitation pulse, the imbalance $R = (S_1 - S_2)/(S_1 + S_2)$ is measured. We retain the part odd under electric field reversal. This method (Bouchiat *et al* 1990, Guéna *et al* 1997) has many advantages. In particular, it is highly selective since it involves the polarization properties of the stimulated emission and thus it guarantees that only 7S atoms excited via the 6S–7S transition contribute. Moreover, the imbalance R is always kept close to zero, that is to say θ^{PV} is detected via a dark field technique. In addition, absolute calibration is performed easily by slightly tilting $\boldsymbol{\epsilon}_{\mathrm{ex}}$ with respect to the polarimeter axes with a calibrated Faraday modulator and hence generating a left–right asymmetry of known magnitude which has the same optical properties as the electroweak asymmetry.

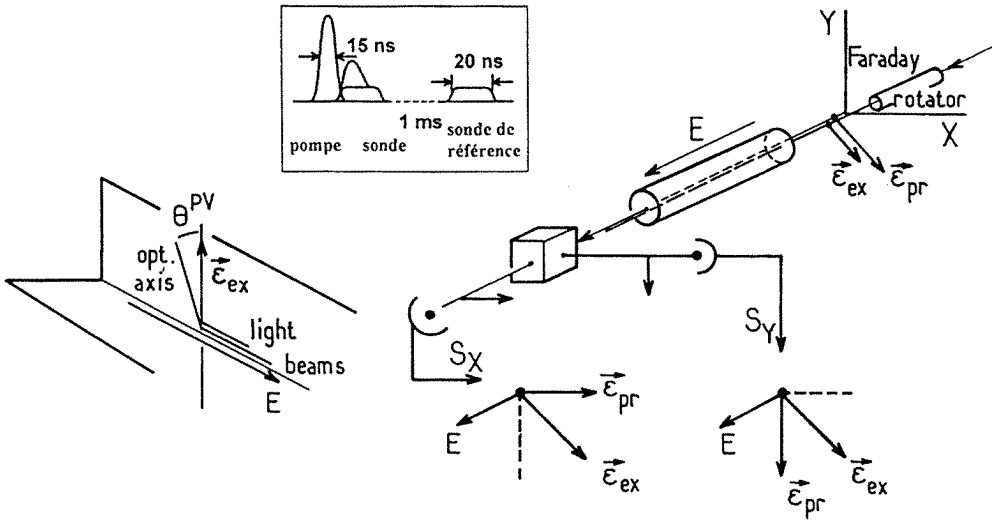

Figure 9. The second generation Paris experiment. Left, the planes of symmetry of the experiment and the deviation of the principle axes from those planes. Bottom right, the two mirror-image configurations leading to a different amplification of the probe. Top right, optical system giving access to the deviation angle θ^{PV} at every individual excitation pulse. Inset: experimental timing.

5.1.2. A radical difference between stimulated emission and fluorescence detection. With respect to fluorescence detection an essential difference, here, is that the left–right asymmetry which appears directly on the transmitted probe beam is amplified with respect to $\theta^{\mathrm{pv}} = -\mathrm{Im}\, E_1^{\mathrm{PV}}/\beta E$ when the optical thickness of the vapour is increased

$$A_{\mathrm{LR}} = \frac{S_1 - S_2}{S_1 + S_2} = -2\theta^{\mathrm{pv}} \left(\exp\left(\mathcal{A}_{\parallel} \left(\frac{\alpha_{\perp} - \alpha_{\parallel}}{2\alpha_{\parallel}} \right) \right) - 1 \right). \tag{38}$$

Here $\mathcal{A}_{\parallel} = \log(I_{\mathrm{out}}^{\mathrm{pr}}/I_{\mathrm{in}}^{\mathrm{pr}})$ is the optical density for the probe and $\alpha_{\perp}, \alpha_{\parallel}$ are the amplification coefficients of the radiation field for the two relative orientations of the pump and probe polarizations. A crucial parameter appearing in formula (28) is the optical anisotropy of the excited medium $\eta = (\alpha_{\perp} - \alpha_{\parallel})/2\alpha_{\parallel}$ which depends only on the hyperfine quantum numbers (F_1, F_2, F_3) of the atomic states $6S_{1/2}$, $7S_{1/2}$, $6P_{3/2}$ involved in the pump-probe transition. The choice $(3, 4, 4)$ with the largest anisotropy leads to the most favourable situation: $\eta = \frac{11}{12}$. It has the additional advantage of involving a 'black state', i.e. not coupled to the probe field, which allows one to work at a high probe intensity without producing a saturation of the asymmetry.

The amplification of the left–right asymmetry which occurs at high optical densities (Bouchiat and Bouchiat 1996) is of considerable value for the optimization of the signal-to-noise ratio. Its attractive feature lies in the fact that all the parameters which lead to an amplification of the optical thickness and hence an amplification of the probe intensity also amplify the asymmetry. Such a characteristic is unusual, since, in all PV Stark experiments based on detection of spontaneous emission, A_{LR} is, to within a numerical factor close to one, equal to $\theta^{\mathrm{pv}} = -\mathrm{Im}E_{\mathrm{pv}}^1/\beta E$, so that a reduction of E which increases the asymmetry is responsible for an unavoidable loss of the fluorescence signal proportional to $\beta^2 E^2$. Here by contrast it is advantageous to increase E for this increases both the signal $I_{\mathrm{out}}^{\mathrm{pr}}$ and the asymmetry A_{LR}. Since $\alpha_{\perp}$ and $\alpha_{\parallel}$ are proportional to the density of excited 7S atoms, hence

to E^2, we see that A_{LR} first grows linearly with E whatever the relative orientation of $\hat{\epsilon}_{\mathrm{pr}}^{\mathrm{in}}$ and $\hat{\epsilon}_{\mathrm{pr}}$, and then much faster, as $(\exp(CE^2) - 1)/E$ in the most favourable polarization configuration.

As for the signal-to-noise ratio, one might be concerned that light amplification generates noise, since the quantum state of the probe field is modified in the amplification process. However, a key point here relies in the experimental procedure retained to measure the asymmetry; in balanced mode operation the variance of the asymmetry can be shown to be always equal to $1/N$ (where N is the average number of detected photons), whatever the quantum state of the light field. The expected amplification of the asymmetry accompanied by a corresponding gain of sensitivity has been verified experimentally.

5.1.3. Present status. With the signal-to-noise ratio presently achieved and the improvements underway (Chauvat *et al* 1997) we can anticipate a precision on θ^{PV} close to 1% for an effective averaging time comparable to that of the 1982–83 experiment. We now consider the crucial problem of systematics. Because the applied electric field is parallel to the excitation beam, it is easily verified (from (27)) that the M_1 and Stark amplitude are in phase quadrature so that the M_1–Stark interference vanishes. It can also be noted that the experiment being performed in a zero magnetic field all the atoms belonging to on hyperfine ground state contribute to the PV effect and the experiment is totally free from any line-shape distortion and line overlapping effects of the kind encountered in the Boulder experiment. However, here a crucial problem can arise in the presence of a longitudinal magnetic field correlated with the applied $\boldsymbol{E}$ field. Actually the atoms can probe such a $H_{z,E_{\mathrm{odd}}}$ field component and allow us to measure it. This component originates from the electric conductivity of the walls of the caesium cell which gives rise to an electric current correlated with the applied voltage generating the $\boldsymbol{E}$-field pulses. Rather than correcting our data for the corresponding systematic effect, a correction which would amount to a fraction of the PV effect, we are working to insulate the internal surface of the cell. We thus expect to make this effect smaller by at least one order of magnitude. Another possible source of systematics comes from the combined effect of transverse electric and magnetic fields. Since the PV effect bears a cylindrical symmetry, while obviously this latter systematic effect does not, there are several possibilities for controlling those effects that we are presently exploring.

For this new experiment we want to stick to the same philosophy adopted in our 1982–83 one (Bouchiat *et al* 1982, 1984), namely to reduce all sources of systematic effects *before* commencing data acquisition. In this way the final result was practically equal to the raw result; no systematic correction was necessary. Of course the realization of a new experimental situation such as the one chosen, which requires high excitation energy density, means the apparition of new physical effects. A complete understanding of all atomic processes present in the condition of the experiment is required and, we believe, is well on the way to being achieved.

5.2. Search for parity violation in a string of isotopes belonging to the same element

5.2.1. Detection in dysprosium using time-resolved quantum beats between nearly crossed levels of opposite parities. There exists in atomic dysprosium ($Z = 66$) a pair of nearly-degenerate levels of opposite parity and of equal angular momentum ($J = 10$). The energy difference is comparable to hyperfine intervals and isotope shifts. These levels, henceforth denoted A and B, are of potential interest for the study of parity violation because this very small energy separation enhances considerably level mixing due to

weak-interaction processes. This system offers the possibility in principle to make PV measurements at a level of precision orders of magnitude better than that achieved so far in other elements.

The scheme of the PV experiment now underway at Berkeley (Budker *et al* 1994, Nguyen *et al* 1997) presents some interesting unusual features. One observes time-resolved Stark-induced quantum beats between levels A and B and looks for interference between the Stark amplitude and the much smaller PV amplitude connecting the two levels. A magnetic field is applied in order to bring Zeeman sublevels with the same value of m_F to near crossing. Now the Stark and PV amplitudes ($\boldsymbol{d}\cdot\boldsymbol{E}$ and H_W) which connect the two opposite parity levels have a relative phase of $\pi/2$, which means that in a static electric field they cannot interfere. Following a suggestion made earlier by Lewis and Williams (1975) for the $2s_{1/2}$, $2p_{1/2}$ hydrogen states, interference can be achieved if one applies a rapidly varying electric field. If the time characteristic of the field variations is short compared to the energy separation Δ divided by $\hbar$, changes in the atomic system are non-adiabatic. The rapid variation of $\boldsymbol{E}$ then provides the right phase adjustment to make the interference possible. More precisely, if all the atoms are initially prepared in the long-lived state B and if the E-field oscillates at the frequency $\omega/2\pi \gg \Delta/h$, the time evolution of the A-state population (with lifetime Γ_A^{-1}) can be expressed as:

$$P_A(t) = \frac{(\boldsymbol{d}\cdot\boldsymbol{E})^2}{\omega^2}\sin^2(\omega t) - \frac{2\boldsymbol{d}\cdot\boldsymbol{E}H_W}{\omega}\frac{\Delta}{\Delta^2+\Gamma_A^2/4}\sin(\omega t).$$

The first term is the quantum beat signal due to Stark mixing at the second harmonic of the electric field frequency. The second term contains the interference between H_W and $\boldsymbol{d}\cdot\boldsymbol{E}$ at the first harmonic frequency. It changes sign with decrossing and the overall sign of the electric and magnetic field. It bears the signature of the T-even pseudoscalar $\mathrm{d}\boldsymbol{E}/\mathrm{d}t\cdot(\boldsymbol{B}-\boldsymbol{B}_c)$ where $\boldsymbol{B}_c$ denotes the magnetic field at the crossing point. The value of H_W is extracted from an analysis of the time dependence of the fluorescence. The most recently published result $|H_W| = 2.3 \pm 2.9(\mathrm{stat}) \pm 0.7(\mathrm{sys})$ Hz is in disagreement with the theoretical prediction of $H_W = 70 \pm 40$ Hz (Dzuba *et al* 1994). Although one has to be aware that in such a complicated atomic system, configuration mixing, the theoretical uncertainty of which may have been underestimated, plays an essential role.

5.2.2. Proposals for experiments in Ba and in Ba-like rare earth elements, Sm and Yb. Barium has nine stable isotopes five of which are even–even nuclei, the most favourable for understanding and calculating nuclear structure corrections to the atomic PV effect. Xiong *et al* (1990) have applied multichannel quantum defect theory to the calculation of the parity-violating E_1 amplitude in several forbidden M_1 transitions of barium ($Z = 56$). The interesting result which comes out of their work is that for the transition $^1S_0(6s^2) \rightarrow {}^3D_1(5d7s)$ (at 305 nm) the magnitude of Im E_1^{pv} is 10 times larger than for the $6S_{1/2} \rightarrow 7S_{1/2}$ Cs transition. The effect is favoured both by a large allowed matrix element connecting the upper state to the nearby state of opposite parity and by configuration mixing effects as well. It is a pity, therefore, that at present there appears to be no planned experimental project and no further atomic calculations in atomic Ba.

On the other hand, several groups have investigated the rare earths elements of outer-shell structure s^2, similar to Ba, but where the more complex overall configuration gives rise to accidental near-degeneracies between levels of opposite parities. In particular an experimental study has been made of the nearly-degenerate, opposite parity Sm states $4f^66s6p\,{}^7G_1$ and $4f^65d6s\,{}^7G_1$ (only 11 cm^{-1} apart), in order to assess the feasibility of using the forbidden M_1 transition from the $4f^66s^2\,{}^7F_0$ ground state to the $4f^65d6s\,{}^7G_1$ state (at

639 nm) for measuring PV effects (Davies *et al* 1989). Discouragingly several experimental difficulties connected with the application of an electric field in a dense Sm vapour looked insurmountable.

On the other hand six M_1 transitions taking place within the ground configuration of samarium were identified as promising candidates for large parity-violating optical rotation (Dzuba *et al* 1986, Barkov *et al* 1989). A great deal of exploratory work has been performed in Oxford to observe those lines whose wavelength was only estimated and to measure several of the oscillator strengths of the allowed transitions relevant for the estimation of the PV effect. Later, the Oxford group searched for the PV optical rotation and finally concluded on the absence of the effect at the level of a few times 10^{-8} for $R = \mathrm{Im}\,(E_1^{\mathrm{pv}}/M_1)$ (Lucas *et al* 1997). They conclude that there is no future for PNC studies on a string of isotopes in these transitions. Several reasons may contribute to the lack of the expected enhancement. The configuration mixings may be unfavourable (see section 2.4.4), the oscillator strengths of the allowed E_1 transitions admixed with the M_1 by the PV mixing may be themselves too small and/or the contribution of the nearby level may be compensated by those of many less adjacent levels.

Nonetheless, the drive to exploit near-degeneracies in rare earths continues. There is in Berkeley a project now starting using ytterbium in the $6s^2\,{}^1S_0 \rightarrow 5d6s^3D_1$ highly forbidden transition. The reason for this choice is the existence of an odd parity state, nearly degenerate with the $5d6s^3D_1$ state ($\Delta E = 600\ \mathrm{cm}^{-1}$). Again this coincidence is supposed to lead to a significant enhancement of the parity mixing amplitude, but, in addition, there is a strong E_1 amplitude between the mixed state and the ground state (DeMille *et al* 1994). The E_1^{pv} amplitude is expected to be 100 times larger than in Cs. Simultaneously there is a Stark-induced amplitude of reasonable magnitude. The effective transition dipole in this case presents a clear similarity with that of caesium (equation (27)). Important exploratory work with an atomic beam of Yb has already been carried out (Bowers *et al* 1996).

5.3. Search for parity violation on a single trapped Ba^+ ion

An entirely new approach has been undertaken in Seattle (Fortson 1993), using the remarkable properties of single trapped ions. In this experiment, a single Ba^+ ion is confined in a radiofrequency trap and laser-cooled so that its residual motion is localized to a small fraction of an optical wavelength. The new feature of this measurement is that the PV signature would be a frequency shift in the ground-state Zeeman splitting. This AC Stark shift is induced by two independent standing-wave laser fields tuned very close to the $6S_{1/2} \rightarrow 5D_{3/2}$, E_2 transition at 2.05 μm. Both beams are derived from the same laser and are incident from perpendicular directions. The spatial phase of the stronger field E' is adjusted so as to provide an antinode at the location of the ion, while that of the second field, with a smaller amplitude E'' is chosen to create a node in the same place. The gradient associated with the E'' field thus drives the quadrupolar electric transition, while the larger E' field, which has no gradient selectively drives the E_1^{pv} transition. It is the interference between the two corresponding amplitudes which gives rise to the PV 'light' shift of the Larmor frequency in the ground state. Reversal properties of this shift reveal the pseudoscalar characteristics of its weak interaction origin. It is convenient to express the observable as an effective magnetic field which is T-even but P-odd:

$$\boldsymbol{B} \propto \langle \boldsymbol{E}' \times (\boldsymbol{\Delta} \times \mathrm{d}\boldsymbol{E}''/\mathrm{d}t)\rangle_t$$

by contrast with a parity-conserving magnetic field which is a pseudovector and, hence, P-even. Here the brackets denote a time-average. The PV Larmor frequency shift is

given by $\Delta\omega_{\mathrm{L}}^{\mathrm{pv}} \simeq 10^{-11} ea_0|E'|/\hbar$, while the much larger parity-conserving quadrupole shift, $\Delta\omega^{\mathrm{quad}} \simeq 10^{-4} ea_0|E''|/\hbar$, is independent of the sublevel. This is of great practical importance in order to render the PV measurement immune from the frequency and amplitude fluctuations of the laser source. An essential requirement for its success is the ability to control the position of a mirror in the proximity of the ion trap so that a standing wave of light can be created with its spatial phase at the ion location controlled to better than $10^{-3}\lambda_{\mathrm{opt}}$.

In this experiment it is expected that the considerable loss accepted on the atomic density as compared to traditional situations, will be compensated by the greatly increased coherence time of the transition (the lifetime of the $5D_{3/2}$ state, $\tau = 50$ s) and by the possibility to tightly focus the laser field at the location of the laser-cooled ion. There is every reason to believe that the atomic calculations in Ba^+ which has the same structure as atomic caesium could be done with just as high accuracy. Therefore the advances of this experimental project are being followed with considerable interest.

5.4. Prospects for PNC measurements in relativistic hydrogenic ions and high-Z helium-like ions

A parity experiment in hydrogen, where no theoretical uncertainty can spoil the result and both the vector and the axial coupling constants of the Z^0 to the proton can be obtained, has remained for decades the most challenging goal in this field, but unfortunately it still seems out of reach (for a condensed review of various attempts see for instance Bouchiat *et al* (1984)).

Although various possibilities for alternative experiments with hydrogenic ions have been discussed in the literature (Dunford 1981, 1986), none seems presently to offer a realistic solution to the observation of a PV effect.

Recently, however, Zolotorev and Budker (1997) have proposed exploiting the developments in relativistic colliders such as high-brightness ion sources and laser-cooling methods in ion storage rings, to devise a new type of experiment. They argue that excitation of the single photon $1S \rightarrow 2S$ transition can be carried out using a heavy ion accelerator such as the SPS or even the LHC. Laser light can be tuned to resonance with the ion transition, using relativistic Doppler tuning. The same technique also provides access to the laser cooling of the ions and polarization of the ions by optical pumping. The authors have discussed the Z-dependence of all the parameters involved in a PV experiment and have focused their attention on the case $Z = 10$ (hydrogen-like Ne ions). They expect that the PV effect could be measured with a statistical uncertainty $\sim 10^{-3}$ in about a week of running time. This is an optimistic conclusion since at this level these measurements provide a quantitative test of the standard model which is sensitive to its various possible extensions.

Another interesting approach consists in using high-Z helium-like ions such as U^{90+}, Th^{88+} or Gd^{62+}. These are systems for which precise calculations of the atomic structure are possible. A suggestion made by Dunford (1996) consists of working with ions in the metastable state $1s_{1/2}2p_{1/2}^3P_0$ with a lifetime long enough that those formed in this state can be extracted from a production target. The weak interaction mixes the $^3P_0$ state with the 2^1S_0 which differs in energy by $\simeq 1$ eV which is a small amount on the scale of the ion level splittings. The parity-mixing amplitude for these states also benefits also from a large-Z enhancement and reaches 5×10^{-6} for He-like uranium. The single-photon decay of the $^3P_0$ state is strictly forbidden because it involves a $J = 0 \rightarrow J = 0$ transition. Dunford (1996) has considered the two-photon decay of this state which involves a parity violating

contribution (with the emission of two E_1 photons) and a parity-conserving amplitude which is a two-photon E_1M_1 transition. Both are characterized by specific dependences on the two-photon directions and polarizations. When the transition probability is computed, pseudoscalar contributions appear in the result. They involve interference between the E_1M_1 and the $2E_1$ amplitudes. The simplest experimental possibility would be to observe the polarization of one of the two photons, averaging over all directions and polarizations of the other photon. In this case, the asymmetry appears as a difference of probabilities for the emission of a right- or a left-circularly polarized photon. However, polarization analysis of hard x-rays being difficult to perform efficiently, it is more interesting to discuss the pseudoscalar asymmetries involved in inducing the transition $2^3P_0 \rightarrow 1^1S_0$ by single-photon stimulated two-photon emission or anti-Stokes Raman scattering. In this case an asymmetry is expected in the rate of the stimulated two-photon emission by reversing the circular polarization of the laser, the polarizations and directions of the x-rays being averaged over. The expected asymmetry is of the order of a few times 10^{-4} which seems most encouraging.

However, we must recognize here that in this section we have accepted leaving momentarily the domain of table-top atomic physics experiments...

5.5. An experimental project to search for an energy difference between two enantiomer molecules

We have discussed theoretically this subject before (see section 2.5). Finding experimental evidence for parity violation in chiral molecules from the observation of an energy difference in the spectrum of the right and left enantiomers is a long-standing dream. Although the idea was first proposed in 1975 by Letokhov, it has only just become technically feasible. Previous attempts to observe such an effect in CHFClBr were blocked by the lack of cleared separated enantiomers of this molecule. Very recently this difficulty has been overcome by French chemists. Such an experiment can now be tried with a real chance of success thanks to the spectacular progress accomplished in the control of CO_2 lasers (Bernard *et al* 1995). The measurements will use a CO_2 laser stabilized to 0.1 Hz on 100 s and will compare the vibration frequencies of the two enantiomers placed in identical chambers (Chardonnet and Bordé, private communication). If the energy shift reaches 1 Hz, as one might expect, the Villetaneuse group should be able to observe it.

6. Conclusion

Low-energy atomic physics experiments still have a role to play in the exploration of the extensions to the standard model. Q_W is a fundamental quantity and high precision measurements cross-checking the most precise recent result are eagerly expected. The dominant uncertainty in the weak charge of the nucleus is now due to the uncertainties in atomic physics calculations. Any gain of accuracy in the determination of Q_W will directly improve the test of electroweak interactions between electrons and atomic nuclei in a region of four-momentum transfer inaccessible to large accelerators. In this way they will place more significant constraints on alternative models, in particular those involving an extra neutral vector boson. The current lepto-quark adventure provides a new illustration of the complementary aspect of the information provided by atomic physics experiments.

With the gain in precision recently achieved on caesium by the Boulder group, the nuclear spin-dependent contribution to the electron–nucleus PV interaction has finally shown-up by comparing different hfs components. Its order of magnitude is roughly

compatible with theoretical predictions in terms of the long sought for nuclear anapole moment. For a detailed interpretation a great deal of work remains to be done both experimentally and theoretically. In future, measurements involving a string of isotopes should open up the path to a direct test of the neutron dependence of the weak charge. Assuming the validity of the standard model, one could obtain from PV measurements unique information about the variation of the neutron distribution along a string of isotopes. Now, it is still an open question as to whether this work can only be performed on atoms with simple structure, or whether better situations may be found in rare earths in spite of their complicated atomic structure.

Atomic physics parity violation has developed into its own field belonging both to elementary particle physics and atomic physics and, against all the odds, met with a series of undisputed successes. The motivations are still so strong that there is every reason to believe that the present impetus in this field will continue. Besides, over the past ten years, atomic physics has developed lots of elegant and potentially powerful new techniques (radiative cooling, atom trapping, light-bound crystals, single-ion spectroscopy, optical quantum noise squeezing). Amongst all this wealth of subtle tools there is a good chance of discovering novel schemes to improve further the precision of parity-violation experiments in atomic and molecular physics. The observation of quantum beats between nearly crossed levels of opposite parity, the detection of a parity-violating light-shift on a single trapped atomic ion (e.g. Ba^+) illuminated by intense laser fields and the search for an energy shift between two enantiomers of a chiral molecule all seem to be very stimulating projects. We expect others to appear and hopefully succeed.

At the same time the collection of results and the progress generated by this activity, both experimental and theoretical, is most impressive. For instance, we have learnt a lot about highly forbidden transitions and their wealth of different transition amplitudes, we can benefit from lots of new spectroscopic properties of exotic (rare earths) atoms, we are learning how to work with francium and radioactive alkali isotopes, we now have at our disposal atomic calculation techniques which, even in a 55 electron system(!), can predict at the percentage level a large variety of basic atomic properties. Without the strong stimulus provided by atomic parity violation, it is hard to imagine how so many interesting but hard-won advances would have been made.

Acknowledgment

We are deeply grateful to M D Plimmer for his careful and critical reading of the manuscript, and for pertinent questions.

References

Adelberger E G, Trainor T A, Fortson E N, Chupp T E, Holmgren D, Iqbal M Z and Swanson H E 1981 *Nucl. Instrum. Methods* **179** 181
Adelberger E G and Haxton W C 1985 *Ann. Rev. Nucl. Part. Sci.* **35** 501
Adloff C *et al* (H1 Collab.) 1997 *Z. Phys.* C **74** 191
Altarelli G 1991 *Phys. Lett.* **261B** 146
Arnison G *et al* (UA1 Collab.) 1983a *Phys. Lett.* **122B** 103
——1983b (UA1 Collab.) *Phys. Lett.* **126B** 398
Avetisov V A, Goldanskii V T and Kuz'min V V 1991 *Physics Today* **44** 33
Banner G *et al* (UA2 Collab.) 1983 *Phys. Lett.* **122B** 476
Barkov L M, Melik-Pashayev D A and Zolotorev M S 1989 *Opt. Spectrosc. (USSR)* **66** 288
Barkov L M and Zolotorev M S 1980 *Sov. Phys.–JETP* **52** 360

Barra A L, Robert J B and Wiesenfeld L 1986 *Phys. Lett.* **115A** 443
——1988 *Europhys. Lett.* **5** 217
Bernard V, Durand P, George T, Nicolaisen H W, Amy-Klein A and Chardonnet C 1995 *IEEE J. Quantum Electron.* **QE-31** 1913
Binetruy P 1994 *Neutral Currents Twenty Years Later (Int. Conf.)* ed U Nguyen-Khac and A Lutz (Singapore: World Scientific) p 233
Birich G N, Bogdanov Yu V, Kanorskii S I, Sobel'man I I, Sorokin V N, Stuck I I and Yukov E A 1984 *Sov. Phys.–JETP* **60** 442
Blundell S A, Hartley A C, Liu Z, Martensson-Pendrill A M and Sapirstein J 1991 *Theor. Chim. Acta* **80** 257
Blundell S A, Johnson W R and Sapirstein J 1990 *Phys. Rev. Lett.* **65** 1411
Blundell S A, Sapirstein J and Johnson W R 1992 *Phys. Rev.* D **45** 1602
Bouchiat C 1991 Private communication
Bouchiat C and Bouchiat M A 1996 *Z. Phys.* D **36** 105–17
Bouchiat C and Piketty C A 1983 *Phys. Lett.* **128B** 73
——1986 *Europhys. Lett.* **2** 511
——1991a *Phys. Lett.* **269B** 195
——1991b *Z. Phys.* C **49** 49
Bouchiat M A and Bouchiat C 1974a *Phys. Lett.* **48B** 111
——1974b *J. Physique* **35** 899–927
——1975 *J. Physique* **36** 493–509
Bouchiat M A and Guéna J 1988 *J. Physique* **49** 2037–44
Bouchiat M A and Pottier L 1986 *Science* **234** 1203
Bouchiat M A, Guéna J, Hunter L and Pottier L 1982 *Phys. Lett.* **117B** 358
——1984 *Phys. Lett.* **134B** 463
——1986 *J. Physique* **47** 1709
Bouchiat M A, Guéna J, Jacquier P, Lintz M and Pottier L 1990 *Opt. Commun.* **77** 374–80
Bouchiat M A, Guéna J and Pottier L 1985a *J. Physique* **46** 1897
Bouchiat M A, Jacquier P, Lintz M and Pottier L 1985b *Opt. Commun.* **56** 100
Bouchiat M A, Poirier M and Bouchiat C 1979 *J. Physique* **40** 1127
Bowers C J, Budker D, Commins E D, DeMille D, Freedman S J, Nguyen A-T, Shang S-Q and Zolotorev M 1996 *Phys. Rev.* A **53** 3103
Breitweg J *et al* (ZEUS Collab.) 1997 *Z. Phys.* C **74** 207
Budker D, DeMille D, Commins E D and Zolotorev M 1983 *Phys. Rev. Lett.* **70** 3019
——1994 *Phys. Lett.* **50A** 132
Chardonnet C and Bordé C 1997 Private communication
Chauvat D, Guéna J, Jacquier P, Lintz M, Bouchiat M A, Plimmer M D and Goodwin C 1997 *Opt. Commun.* **138** 249
Chen B Q and Vogel P 1993 *Phys. Rev.* C **48** 1392
Cho D, Wood C S, Bennett S C, Roberts J L and Wieman C E 1997 *Phys. Rev.* A **55** 1007
Commins E D 1981 *Atomics Physics 7* ed D Kleppner and F M Pipkin (New York: Plenum) p 121
——1987 *Phys. Scr.* **36** 468
Curtis-Michel F 1965 *Phys. Rev.* B **138** 408
Davies I O G, Baird P E G, Sandars P G H and Wolfenden T D 1989 *J. Phys. B: At. Mol. Opt. Phys.* **22** 741
DeMille D 1995 *Phys. Rev. Lett.* **74** 4165
DeMille D, Budker D and Commmins E D 1994 *Phys. Rev.* A **50** 4657
Desplanques B, Donaghue J F and Holstein B R 1980 *Ann. Physics* **124** 449
Dmitriev V F, Khriplovich I B and Telitsin V B 1994 *Nucl. Phys.* A **577** 691
Dmitriev V F and Telitsin V B 1997 *Nucl. Phys.* A **613** 237
Drell P S and Commins E D 1984 *Phys. Rev. Lett.* **53** 968
——1985 *Phys. Rev.* A **32** 2196
Dunford R W 1981 *Phys. Lett.* **99B** 58
——1986 *Phys. Rev.* A **33** 2949
——1996 *Phys. Rev.* A **54** 3820
Dzuba V A, Flambaum V V and Khriplovich I 1986 *Z. Phys.* D **1** 243
Dzuba V A, Flambaum V V and Kozlov M G 1994 *Phys. Rev.* A **50** 3812
Dzuba V A, Flambaum V V, Kraftmakher A Y and Sushkov O P 1989a *Phys. Lett.* **142A** 373
Dzuba V A, Flambaum V V, Silvestrov P G and Sushkov O P 1987 *J. Phys. B: At. Mol. Phys.* **20** 3297
——1988 *Europhys. Lett.* **7** 413

Dzuba V A, Flambaum V V and Sushkov O P 1989 *Phys. Lett.* **141A** 147
——1995 *Phys. Rev.* A **51** 3454
Edwards J N H, Phipp S J, Baird P E G and Nakayama S 1995 *Phys. Rev. Lett.* **74** 2654–7
Fayet P 1977 *Phys. Lett.* **69B** 489
——1979 *Phys. Lett.* **84B** 416
——1980 *Phys. Lett.* **96B** 83
——1986a *Phys. Lett.* **171B** 261
——1986b *Phys. Lett.* **172B** 363
——1986c *Nucl. Phys.* B **187** 184
——1990 *Nucl. Phys.* B **347** 743
Flambaum V V and Khriplovich I B 1980 *Sov. Phys.–JETP* **52** 835
Flambaum V V and Murray D W 1997 *Phys. Rev.* C **56** 1641
Flambaum V V and Vorov O K 1994 *Phys. Rev.* C **49** 1827
——1995 *Phys. Rev.* C **51** 1521
Flambaum V V, Khriplovich I B and Sushkov O P 1984 *Phys. Lett.* **146B** 367
Fortson E N 1993 *Phys. Rev. Lett.* **70** 2383
Fortson E N, Pang Y and Wilets L 1990 *Phys. Rev. Lett.* **65** 2857
Frantsuzov P A and Khriplovich I B 1988 *Z. Phys.* D **7** 297
Gajzago E and Marx G 1974 *Atomki Közl. Suppl.* **16** 177
Gilbert S L, Noeker M C, Watts R N and Wieman C E 1985 *Phys. Rev. Lett.* **55** 2680
Glashow S L 1961 *Nucl. Phys.* **22** 579
Guéna J, Chauvat D, Jacquier P, Lintz M, Plimmer M D and Bouchiat M A 1997 *J. Opt. Soc. Am.* B **14** 271–84
Gwinner G, Behr J A, Cahn S B, Ghosh A, Orozco L A, Sfrouse G D and Xu F 1994 *Phys. Lett.* **72** 3795
Hartley A C and Sandars P G H 1990 *J. Phys. B: At. Mol. Opt. Phys.* **23** 2649
Hasert F J *et al* 1973 *Phys. Lett.* **46B** 138
Haxton W C, Henley E M and Musolf M J 1989 *Phys. Rev. Lett.* **63** 949
Hegstrom R and Kondepudi D K 1990 *Sci. Am.* **262** 98
Hegstrom R A, Rein D W and Sandars P G H 1989 *J. Chem. Phys.* **73** 2329
Hinds E A 1980 *Phys. Rev. Lett.* **44** 374
——1988 *The Spectrum of Atomic Hydrogen Advances (Advanced Series on Directions in High Energy Physics)* ed G W Series (Singapore: World Scientific)
Hollister J H, Apperson G R, Lewis L L, Emmons T P, Vold T G and Fortson E N 1981 *Phys. Rev. Lett.* **46** 642
Itzykson C and Zuber J B 1980 *Quantum Field Theory* (New York: McGraw-Hill)
Kambara H S *et al* (CDF Collab) 1997 Search for leptoquarks at CDF hep-ex/9706026 27 June 1997 *Proc. Hadron Collider Physics XII (Stony Brook June 1997)* to be published
Khriplovich I B 1974 *JETP Lett.* **20** 315
Kondepudi D K and Nelson G W 1985 *Nature* **314** 438
Kozlov M G 1988 *Phys. Lett.* **130A** 426
Kraftmakher A Y 1988 *Phys. Lett.* **132A** 167
Langacker P and Luo M 1992 *Phys. Rev.* D **45** 278
Lee B W 1972 *Phys. Rev.* D **6** 1188
Lee T D and Yang C N 1956 *Phys. Rev.* **104** 254
Letokhov V S 1975 *Phys. Lett.* **53A** 275
Levy L P and Williams W L 1982 *Phys. Rev. Lett.* **48** 607
Lewis R R and Williams W L 1975 *Phys. Lett.* **59B** 70
Liu Z and Johnson W R 1987 *Phys. Lett.* **119A** 407
Lu Z-T, Bowers C J, Freedman S J, Fujikawa B K, Mortara J L, Shang S-Q, Coulter K P and Young L 1994 *Phys. Rev. Lett.* **72** 3791
Lu Z-T, Corwin K L, Vogel K R, Wieman C E, Dinneen T P, Maddi J and Gould H 1997 *Phys. Rev. Lett.* **79** 994
Lucas D M, Warrington R B and Stacey D N 1997 A search for parity violation in atomic samarium *Phys. Rev.* A submitted
Macpherson M J D, Zetie K P, Warrington R B, Stacey D N and Hoare J P 1991 *Phys. Rev. Lett.* **67** 2784
Marciano W and Sirlin A 1984 *Phys. Rev.* D **29** 75
Mason S F 1984 *Nature* **311** 19
Meekhof D M, Vetter P, Majumder P K, Lamoreaux S K and Fortson E N 1993 *Phys. Rev. Lett.* **71** 3442
Neuffer D and Commins E D 1977 *Phys. Rev.* A **16** 844
Nguyen A T, Budker D, DeMille D and Zolotorev M 1997 Search for parity non-conservation in atomic dysprosium *Phys. Rev.* A to appear

Noecker M C, Masterson B P and Wieman C E 1988 *Phys. Rev. Lett.* **61** 310
Norman D *et al* (DO Collab) 1997 Search for leptoquarks at d0 hep-ex/9706027 30 Jun 1997 *Proc. Hadron Collider Physics XII* to be published
Peskin M E and Takeuchi T 1992 *Phys. Rev.* D **46** 381
Pollock S J, Fortson E N and Wilets L 1992 *Phys. Rev.* C **46** 2587
Prentki J and Zumino B 1972 *Nucl. Phys.* B **47** 99
Prescott C Y *et al* 1978 *Phys. Lett.* **77B** 347
——1979 *Phys. Lett.* **84B** 524
Rein D W, Hegstrom R A and Sandars P G H 1979 *Phys. Lett.* **71A** 499
Rubbia A *et al* 1994 *Neutral Currents Twenty Years Later (Int. Conf.)* ed U Nguyen-Khac and A Lutz (Singapore: World Scientific) p 309
Salam A 1968 *Elementary Particle Theory: Relativistic Groups and Analyticity (8th Nobel Symp.)* ed N Svartholm (Stockholm: Almqvist and Wicksell) p 367
Sandars P G H 1975 *Atomics Physics 4* ed G zu Putlitz, E Weber and A Winnacker (New York: Plenum) p 399
——1987 *Phys. Scr.* **36** 904
Simsarian J E, Gwinner A G G, Orozco L A, Sprouse G D and Voytas P A 1996 *Phys. Rev. Lett.* **76** 3522
Stacey D 1992 *Phys. Scr.* **40** 15
Sushkov O P and Telitsin V B 1993 *Phys. Rev.* C **48** 1069
Suzuki T *et al* 1995 *Phys. Rev. Lett.* **75** 3241
't Hooft G 1971a *Nucl. Phys.* B **33** 173
——1971b *Nucl. Phys.* B **35** 167
Tanner C and Commins E D 1986 *Phys. Rev. Lett.* **56** 332
Vetter P, Meekhof D M, Majumder P K, Lamoreaux S K and Fortson E N 1995 *Phys. Rev. Lett.* **74** 2658
Vieira D J 1994 private communication
VMB Collab. 1995 Expérience PS 203, LEAR *CERN Courier* June p 13
Warrington R B, Thompson C D and Stacey D N 1993 *Europhys. Lett.* **24** 641
Weinberg S 1967 *Phys. Rev. Lett.* **19** 1264
Wieman C E, Noecker M C, Masterson B P and Cooper J 1987 *Phys. Rev. Lett.* **58** 1738
Wood C S, Bennett S C, Cho D, Masterson B P, Roberto J L, Tanner C E and Wieman C E 1997 *Science* **275** 1759
Wu C S 1957 *Phys. Rev.* **105** 1413
Xiong X, He M, Zhao Y and Zhang Z 1990 *J. Phys. B: At. Mol. Opt. Phys.* **23** 4329
Zel'dovich Y B 1957 *Sov. Phys.–JETP* **6** 1184
——1959 *Sov. Phys.–JETP* **9** 682
Zhao W Z, Simsarian J E, Orozco L A, Shi W and Sfrouse G D 1997 *Phys. Rev. Lett.* **78** 4169
Zolotorev M and Budker D 1997 *Phys. Rev. Lett.* **78** 4717